Alignment-free method for DNA sequence clustering using Fuzzy integral similarity

Ajay Kumar Saw[1], Garima Raj[2], Manashi Das[3], Narayan C. Talukdar[4], Binod Chandra Tripathy[5] and Soumyadeep Nandi[6,]*

[1] Mathematical Sciences Division, Institute of Advanced Study in Science and Technology, Guwahati-35, India.

[2,3,4,6] Life Science Division, Institute of Advanced Study in Science and Technology, Guwahati-35,

India.

[5] Mathematics Department, Tripura University, Tripura, India.

* To whom correspondence should be addressed. Email: soumyadeep.nandi@gmail.com; snandi@iasst.gov.in

ROC_supplementary material

Explanation:

The objective of the study is to develop an Alignment-free tool for sequence clustering. To illustrate the effectiveness of our method we compared the distance matrices and the phylogenetic trees generated by our method with the other freely available recent alignment-free tools [1]. The clustering efficiency of our tool can be noticed across all the benchmark datasets. The phylogenetic trees generated by our method and the other freely available recent methods shows superiority of our method over the other methods in terms of sequence clustering. The consistency can also be seen from the statistical analysis such as AUC (area under the ROC) values calculated from ROC (Receiver operating characteristic) curves. AUC values are often used to explain the accuracy of models and not to compare them. Accuracy classification of AUC is summarised in Table 1, which is given below.

AUC Range	**Classification**
AUC ≥ 0.9	high accuracy
0.7 ≤ AUC< 0.9	moderate accuracy
0.5 ≤ AUC< 0.7	Low accuracy

Table 1: Accuracy classification of AUC [2, 3, 4, 5, 6].

A low AUC value does not necessarily imply a bad or poor model; rather it simply suggests that, besides the accounted predictors, other factors also exercise influence on the response variable. It is evident from the ROC plots below that our method's performance is in good agreement with other methods.

ROC calculation:-

The phylogenetic tree is generated by a distance matrix using PHYLIP package [7] which is equal to (1-similarity matrix) from equation (12) in our manuscript. We used similarity matrix for ROC analysis. We follow sonego et al.'s method [8] for calculating the ROC. In the similarity matrix, we put positive sign, if the two sequences belong to same class (i.e., genus level classification, phylum level classification, family level classification, etc.,) otherwise we put negative sign. We plotted the ROC curve by changing the decision threshold in either strictly increasing or strictly decreasing pattern lies between the minimum and maximum values of the similarity matrix. We plotted the FPR (false positive rate) on X-axis and TPR (true positive rate) on Y-axis. Every point in the ROC curve corresponds to a discrete classifier that can be calculated using a decision threshold (Figure 3 in [8]). After plotting ROC curve, we calculated the area under the ROC curve (AUC).

Phylogenetic tree on 11 AMF sequences.

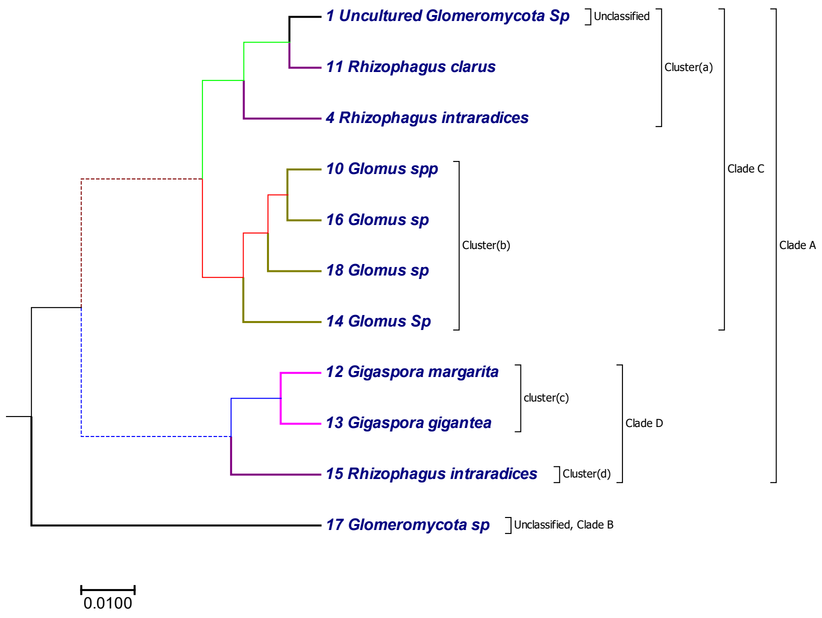

Figure 1: Our method.

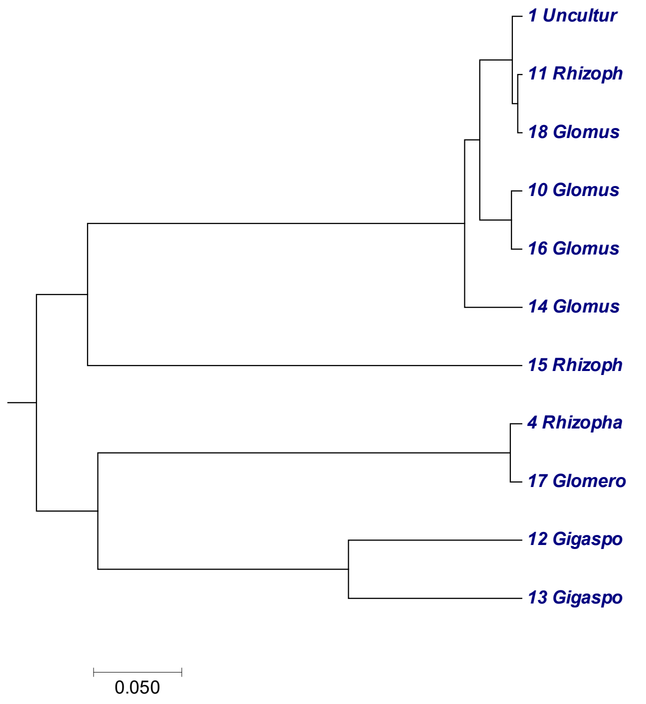

Figure 2 : CV method using string length 3.

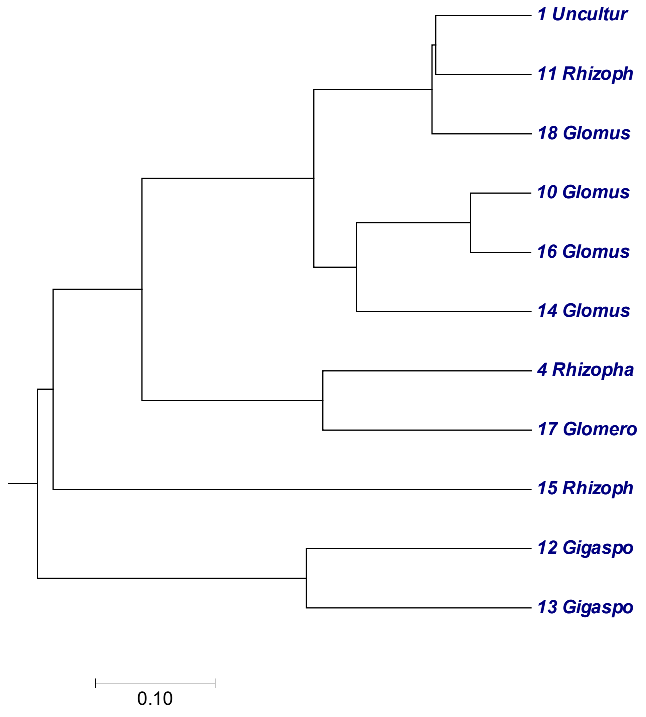

Figure 3: FFP method using string length 7.

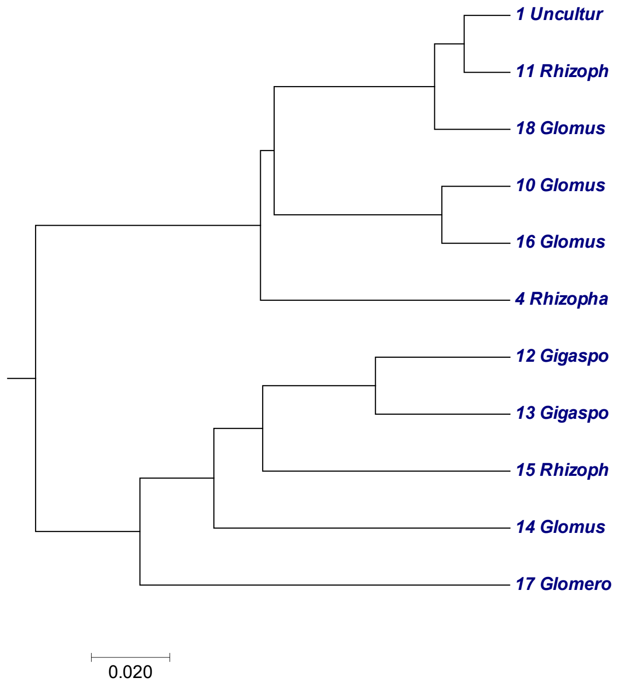

Figure 4: RTD method using string length 1.

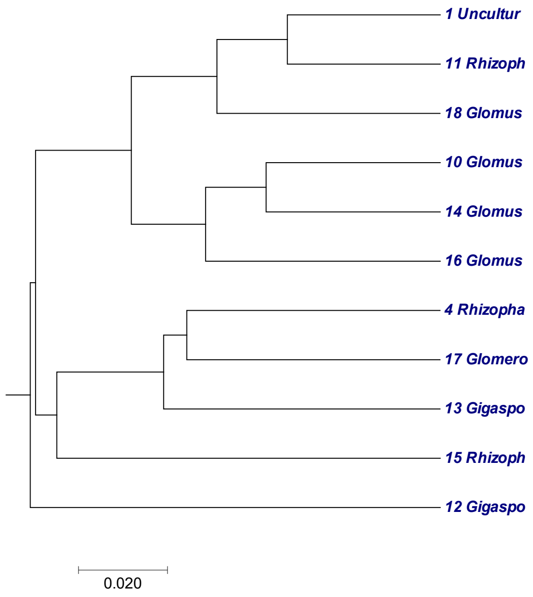

Figure 5: BBC method.

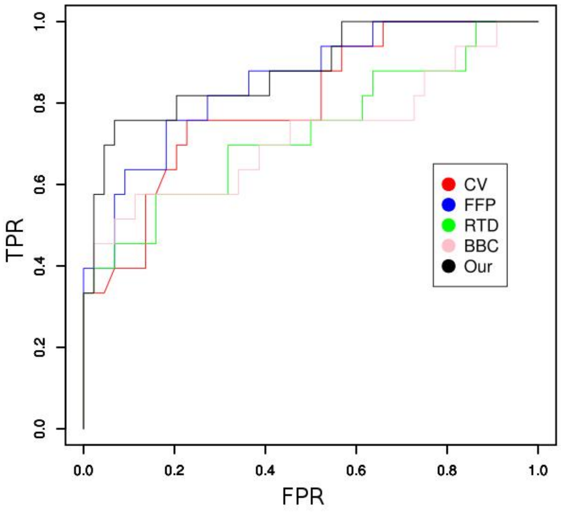

Dataset→ 11 AMF		
Methods↓	**AUC↓**	**Running time↓**
CV method	0.796143	<1s
FFP method	0.85124	<1s
RTD method	0.727273	<1s
BBC method	0.720386	<1s
Our method	0.880165	<1s

Figure 6: Receiver operating characteristic curve (ROC) and Area under the ROC Curve on 11 AMF sequences.

The phylogenetic tree (Figure 1) generated by our method successfully clustered all glomus genera (cluster (b)) belonging to family glomeraceae, all gigaspora genera (cluster (c)) belonging to family gigasporaceae and all rhizophagus genera (cluster (a)) belonging to family glomeraceae except 15 Rhizophagus intraradice (cluster (d)) in separate clades. While comparing the tree prepared by our method (Figure 1) with the tree prepared by other freely available tools [1] (Figures 2, 3, 4 and 5). We found that, all glomus genera were not properly clustered together in Figures 2, 3, 4 and 5. Similarly, all gigaspora genera were not clustered together in Figure 5. This shows the advantage of our method over others in terms of sequence clustering. Moreover, the AUC of our method is 0.88 (Figure 6), which indicates that our method has moderate accuracy (Table 1).

Phylogenetic tree on 41 mammalian sequences.

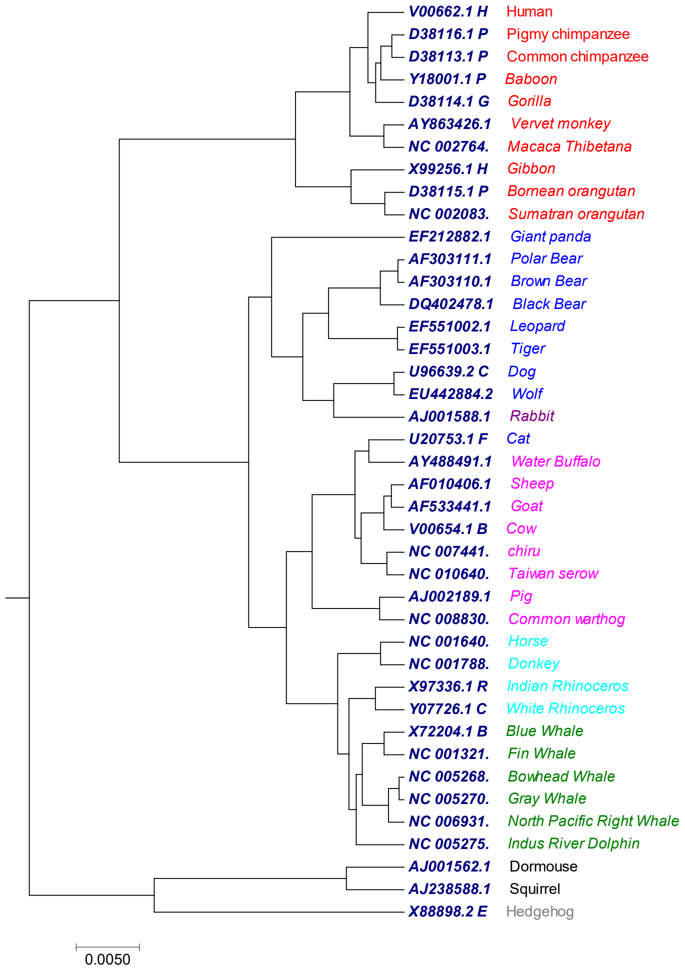

Figure 7: Our method.

(Primates (red), Cetacea (green), Artiodactyla (pink), Perissodactyla (light green), Rodentia (black), Lagomorpha (dark red), Carnivore (blue), and Erinaceomorpha (grey)).

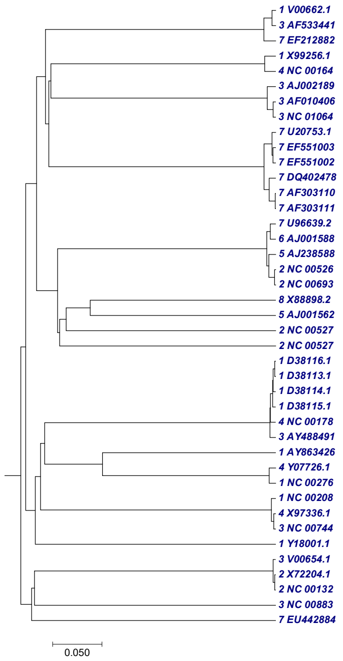

Figure 8: CV method using string length 3.

(1 → Primates, 2 → Cetacea, 3 → Artiodactyla, 4 → Perissodactyla, 5 → Rodentia, 6 → Lagomorpha, 7 → Carnivore, and 8 → Erinaceomorpha).

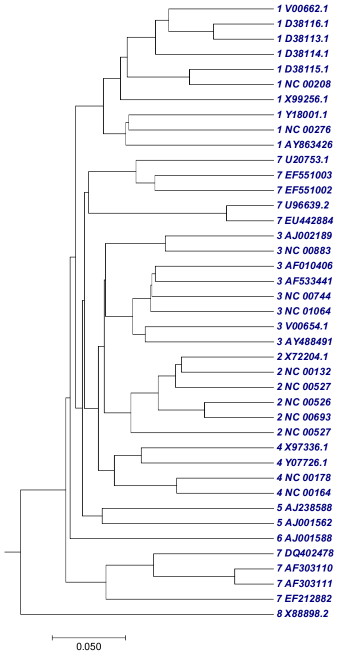

Figure 9: FFP method using string length 7.

(1 → Primates, 2 → Cetacea, 3 → Artiodactyla, 4 → Perissodactyla, 5 → Rodentia, 6 → Lagomorpha, 7 → Carnivore, and 8 → Erinaceomorpha).

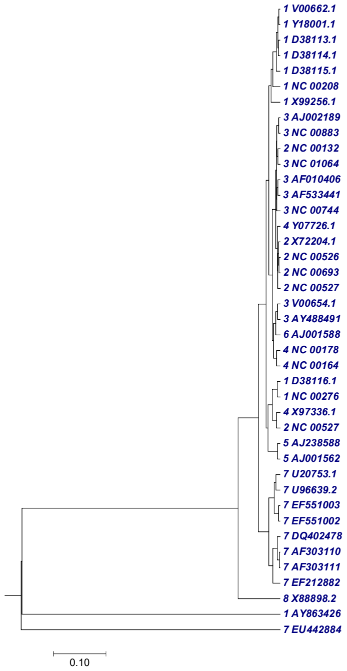

Figure 10: RTD method using string length 1.

(1 → Primates, 2 → Cetacea, 3 → Artiodactyla, 4 → Perissodactyla, 5 → Rodentia, 6 → Lagomorpha, 7 → Carnivore, and 8 → Erinaceomorpha).

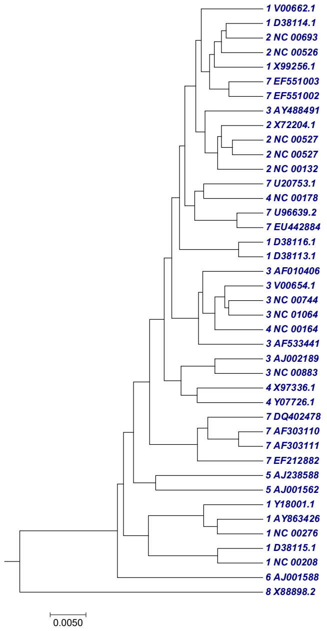

Figure 11: BBC method.

1→ Primates, 2 → Cetacea, 3 → Artiodactyla, 4 → Perissodactyla, 5 → Rodentia, 6 → Lagomorpha, 7 → Carnivore, and 8 → Erinaceomorpha).

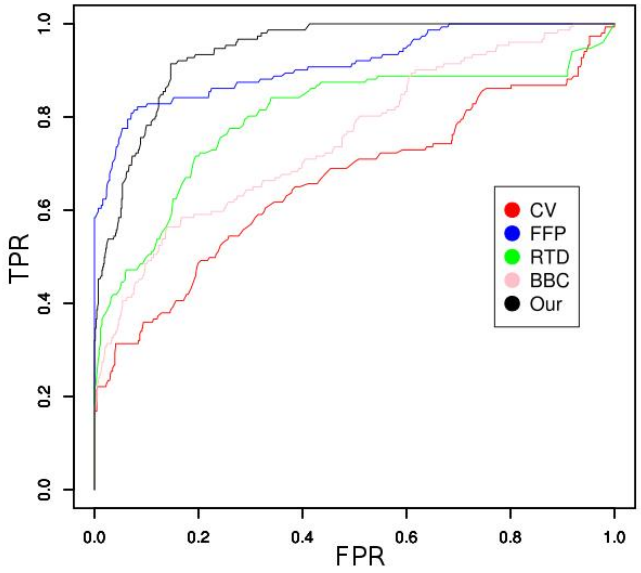

Dataset→ 41 mammalian		
Methods↓	**AUC↓**	**Running time ↓**
CV method	0.65962	<1s
FFP method	0.912888	1s
RTD method	0.795208	<1s
BBC method	0.753803	5s
Our method	0.940862	<1s

Figure 12: Receiver operating characteristic curve (ROC) and Area under the ROC Curve on 41 mammalian sequences.

41 species in the phylogenetic tree (Figure 7) generated by our approach, were correctly divided into eight groups: Primates (red), Cetacea (green), Artiodactyla (pink), Perissodactyla (light green), Rodentia (black), Lagomorpha (dark red), Carnivore (blue), and Erinaceomorpha (grey). The cat species in our approach was clustered with the Artiodactyla group. We compared the phylogenetic tree (Figure 7) generated by our approach with the phylogenetic tree (Figures 8, 9, 10 and 11) prepared by other freely available tools [1]. In Figure 8, eight groups were not properly clustered. In Figures 10 and 11, Primates (1), Cetacea (2), Artiodactyla (3), Perissodactyla (4) were all divided into more than one group. Figure 9 has similarity with our result (Figure 7). This shows the advantage of our method over other methods (Figures 8, 10 and 11) in terms of sequence clustering. Moreover, the AUC of our method is 0.94 (Figure 12), which indicates that our method has high accuracy (Table 1).

Phylogenetic tree on 59 ebolavirus sequences.

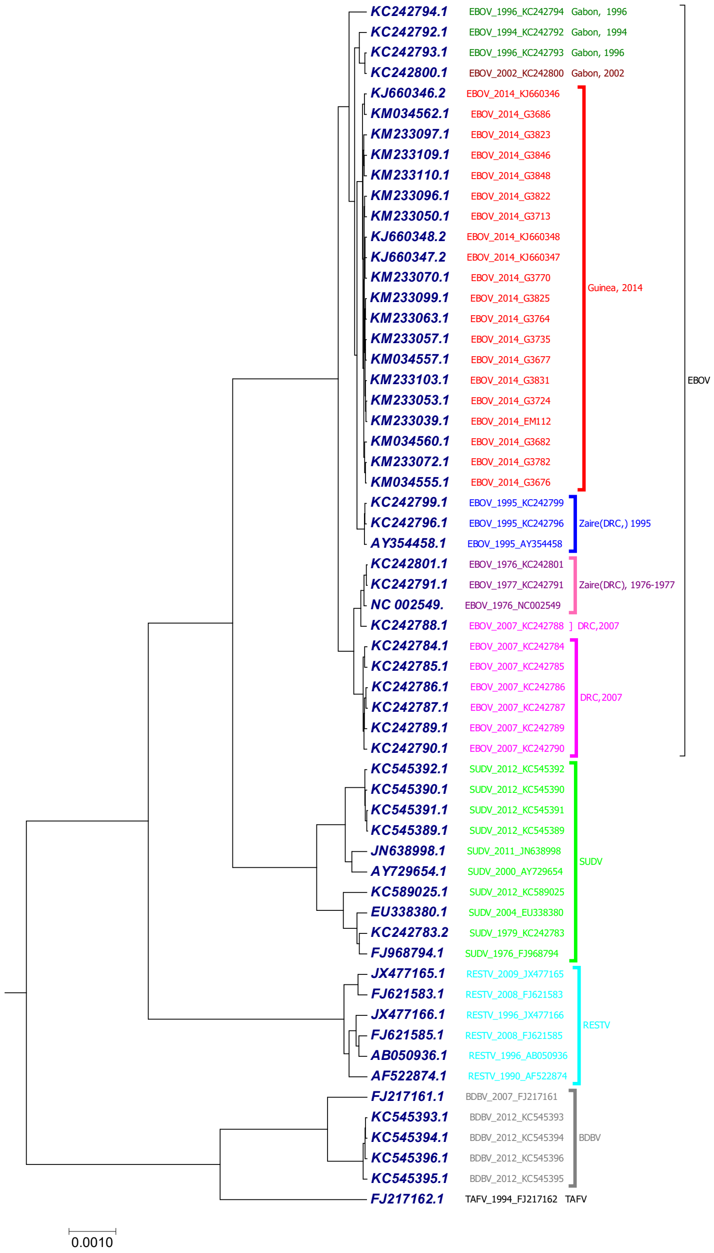
KC242794.1 EBOV_1996_KC242794 Gabon, 1996
KC242792.1 EBOV_1994_KC242792 Gabon, 1994
KC242793.1 EBOV_1996_KC242793 Gabon, 1996
KC242800.1 EBOV_2002_KC242800 Gabon, 2002
KJ660346.2 EBOV_2014_KJ660346
KM034562.1 EBOV_2014_G3686
KM233097.1 EBOV_2014_G3823
KM233109.1 EBOV_2014_G3846
KM233110.1 EBOV_2014_G3848
KM233096.1 EBOV_2014_G3822
KM233050.1 EBOV_2014_G3713
KJ660348.2 EBOV_2014_KJ660348
KJ660347.2 EBOV_2014_KJ660347
KM233070.1 EBOV_2014_G3770
KM233099.1 EBOV_2014_G3825
KM233063.1 EBOV_2014_G3764
KM233057.1 EBOV_2014_G3735
KM034557.1 EBOV_2014_G3677
KM233103.1 EBOV_2014_G3831
KM233053.1 EBOV_2014_G3724
KM233039.1 EBOV_2014_EM112
KM034560.1 EBOV_2014_G3682
KM233072.1 EBOV_2014_G3782
KM034555.1 EBOV_2014_G3676
Guinea, 2014
KC242799.1 EBOV_1995_KC242799
KC242796.1 EBOV_1995_KC242796
AY354458.1 EBOV_1995_AY354458
Zaire(DRC,) 1995
KC242801.1 EBOV_1976_KC242801
KC242791.1 EBOV_1977_KC242791
NC 002549. EBOV_1976_NC002549
Zaire(DRC), 1976-1977
KC242788.1 EBOV_2007_KC242788] DRC,2007
KC242784.1 EBOV_2007_KC242784
KC242785.1 EBOV_2007_KC242785
KC242786.1 EBOV_2007_KC242786
KC242787.1 EBOV_2007_KC242787
KC242789.1 EBOV_2007_KC242789
KC242790.1 EBOV_2007_KC242790
DRC,2007
EBOV
KC545392.1 SUDV_2012_KC545392
KC545390.1 SUDV_2012_KC545390
KC545391.1 SUDV_2012_KC545391
KC545389.1 SUDV_2012_KC545389
JN638998.1 SUDV_2011_JN638998
AY729654.1 SUDV_2000_AY729654
KC589025.1 SUDV_2012_KC589025
EU338380.1 SUDV_2004_EU338380
KC242783.2 SUDV_1979_KC242783
FJ968794.1 SUDV_1976_FJ968794
SUDV
JX477165.1 RESTV_2009_JX477165
FJ621583.1 RESTV_2008_FJ621583
JX477166.1 RESTV_1996_JX477166
FJ621585.1 RESTV_2008_FJ621585
AB050936.1 RESTV_1996_AB050936
AF522874.1 RESTV_1990_AF522874
RESTV
FJ217161.1 BDBV_2007_FJ217161
KC545393.1 BDBV_2012_KC545393
KC545394.1 BDBV_2012_KC545394
KC545396.1 BDBV_2012_KC545396
KC545395.1 BDBV_2012_KC545395
BDBV
FJ217162.1 TAFV_1994_FJ217162 TAFV
0.0010

Figure 13: Our method.

(Bundibugyo virus (BDBV), Reston virus (RESTV), Ebola virus (EBOV), Sudan virus (SUDV), and Tai Forest virus (TAFV)).

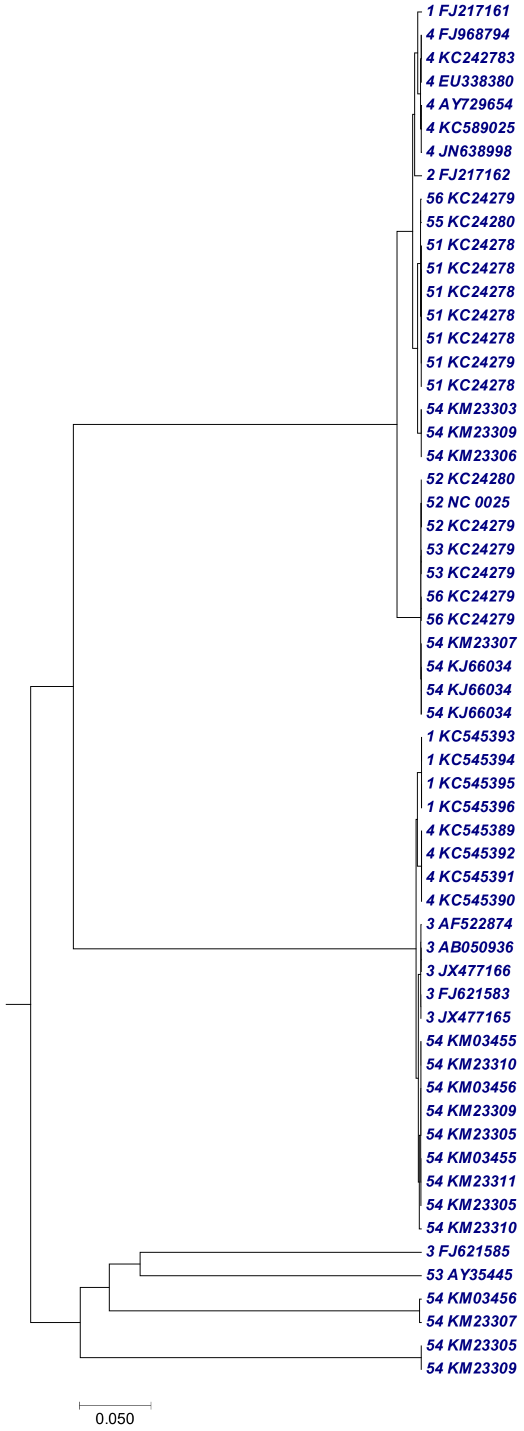

Figure 14: CV method using string length 3.

(1 →Bundibugyo virus (BDBV), 2 →Tai Forest virus (TAFV)), 3 →Reston virus (RESTV), 4 →Sudan virus (SUDV), 51,51,53,54,55 and 56 →Ebola virus (EBOV)).

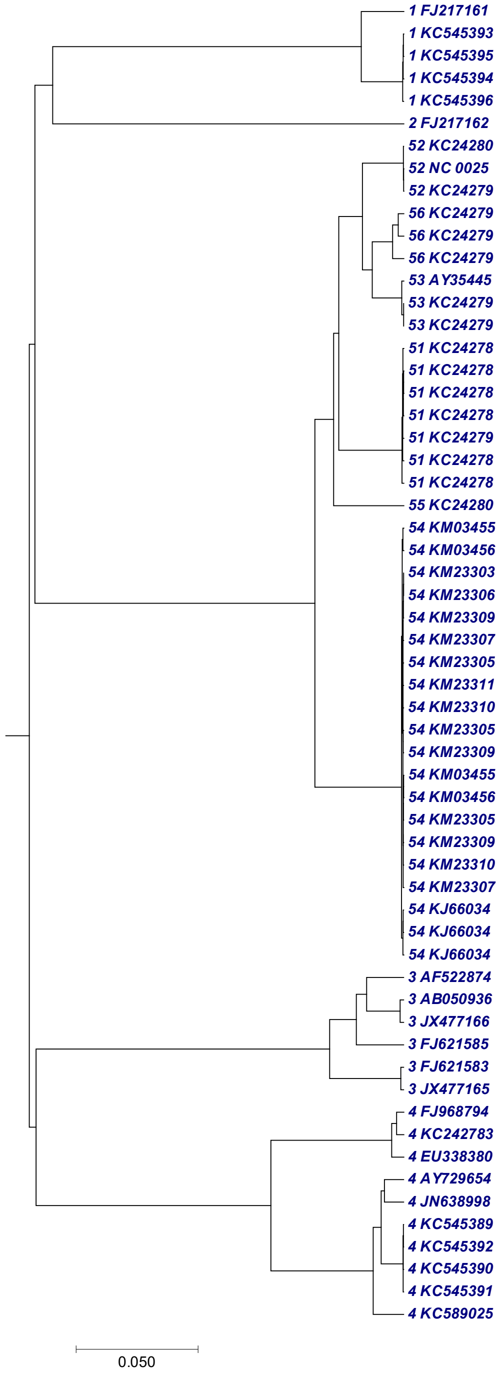

Figure 15: FFP method using string length 7.

(1 →Bundibugyo virus (BDBV), 2 →Tai Forest virus (TAFV)), 3 →Reston virus (RESTV), 4 →Sudan virus (SUDV), 51,51,53,54,55 and 56 →Ebola virus (EBOV)).

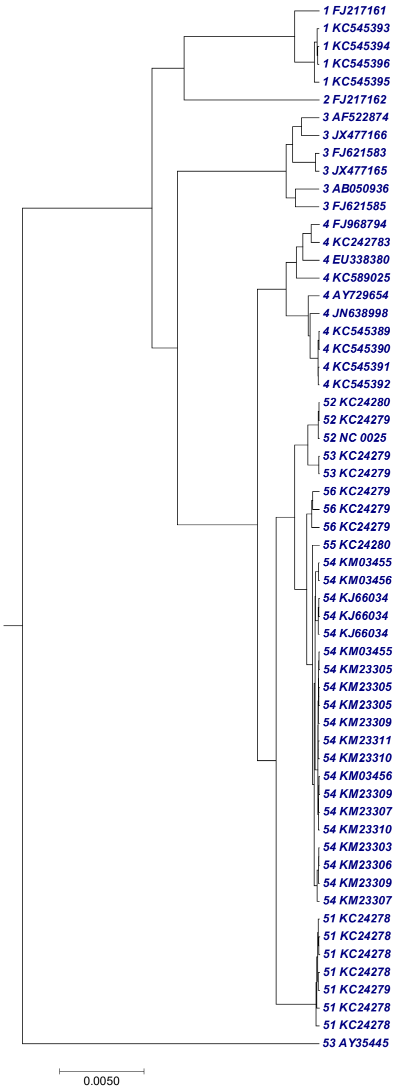

Figure 16: RTD method using string length 1.

(1 →Bundibugyo virus (BDBV), 2 →Tai Forest virus (TAFV)), 3 →Reston virus (RESTV), 4 →Sudan virus (SUDV), 51,51,53,54,55 and 56 →Ebola virus (EBOV)).

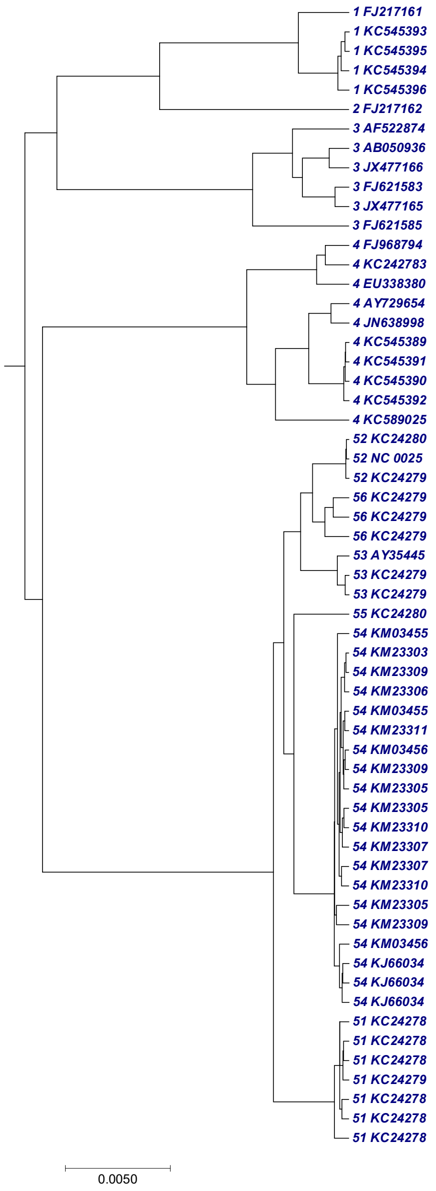

Figure 17: BBC method.

(1 →Bundibugyo virus (BDBV), 2 →Tai Forest virus (TAFV)), 3 →Reston virus (RESTV), 4 →Sudan virus (SUDV), 51,51,53,54,55 and 56 →Ebola virus (EBOV)).

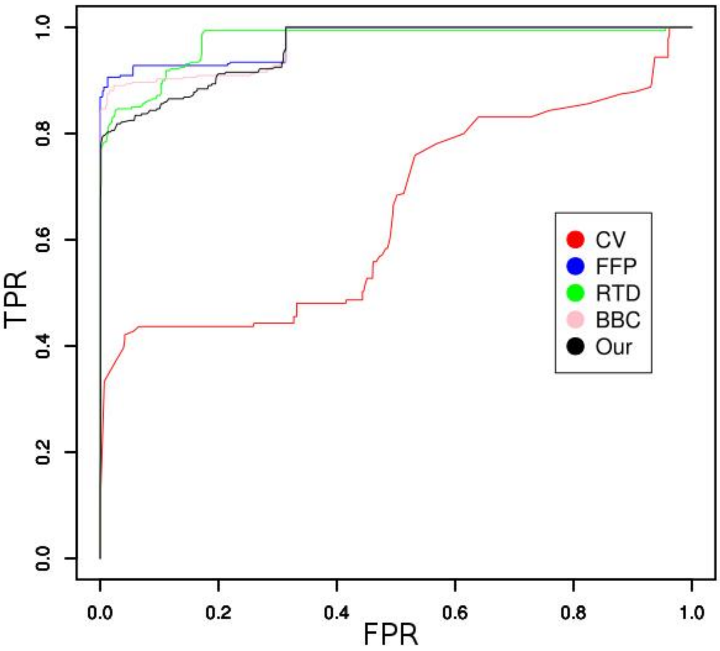

Dataset→ 59 ebolavirus		
Methods↓	**AUC↓**	**Running time↓**
CV method	0.644968	<1s
FFP method	0.976518	1s
RTD method	0.973445	<1s
BBC method	0.969714	7s
Our method	0.959937	<1s

Figure 18: Receiver operating characteristic curve (ROC) and Area under the ROC Curve on 59 ebolavirus sequences.

The Ebolavirus genus includes five species: Bundibugyo virus (BDBV), Reston virus (RESTV), Ebola virus (EBOV), Sudan virus (SUDV), and Tai Forest virus (TAFV). As shown in Figure 13 generated by our method, the five species were correctly separated. We compared the phylogenetic tree (Figure 13) generated by our approach with the phylogenetic trees (Figures 14, 15, 16 and 17) prepared by other freely available tools [1]. In Figure 14, five species were not properly clustered. Similarly, our result (Figure 13) was in consensus with Figures 15, 16 and 17. Moreover, the AUC of our method is 0.96 (Figure 18), which indicates that our method has high accuracy (Table 1).

Phylogenetic tree on 30 coronavirus sequences.

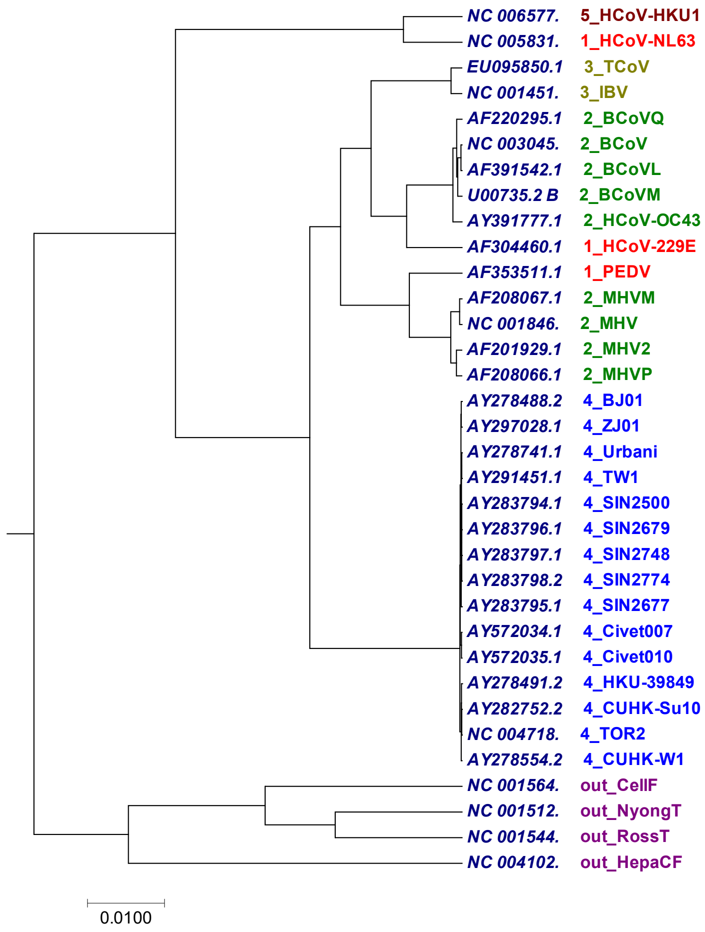

Figure 19: Our method.

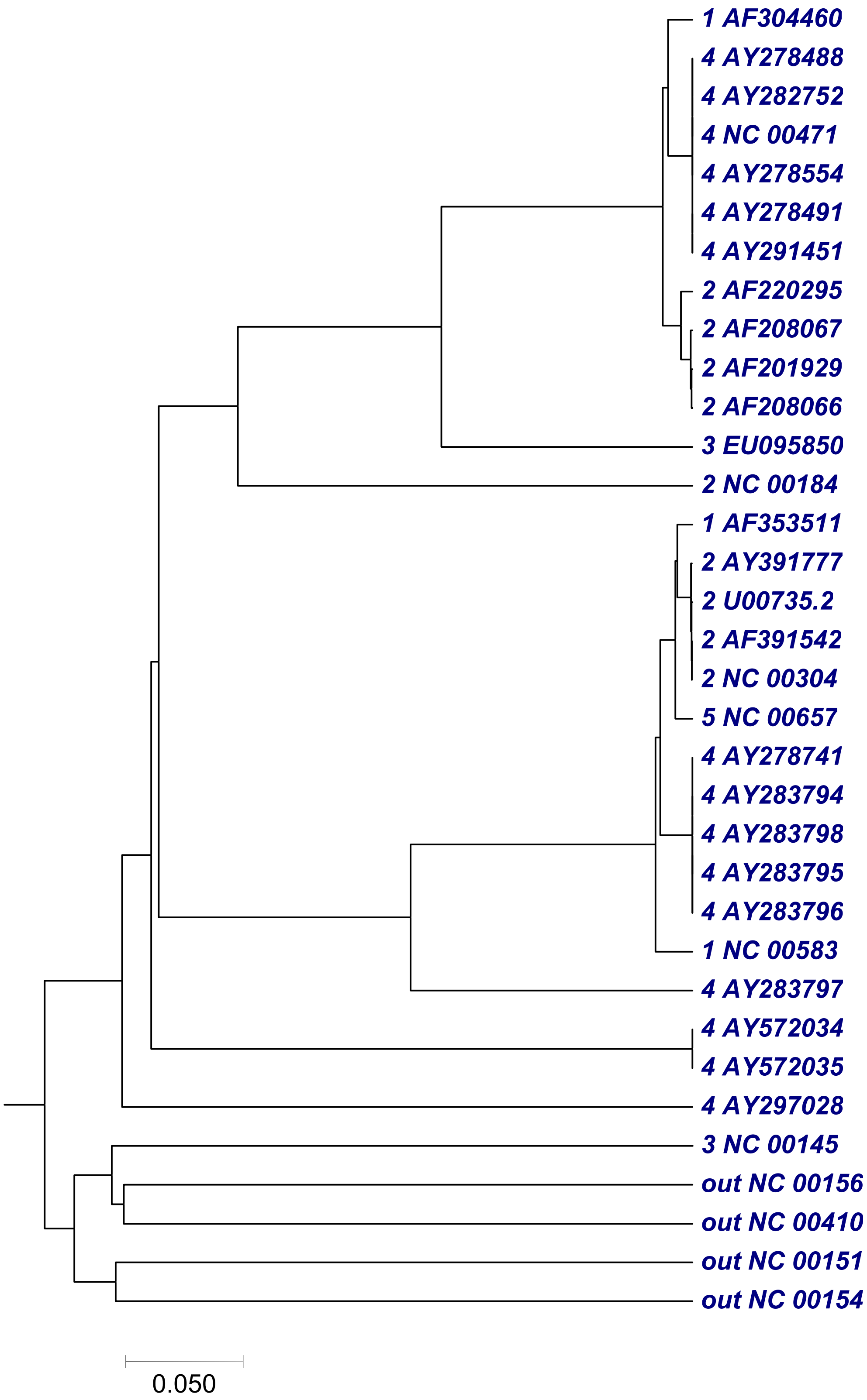

Figure 20: CV method using string length 3.

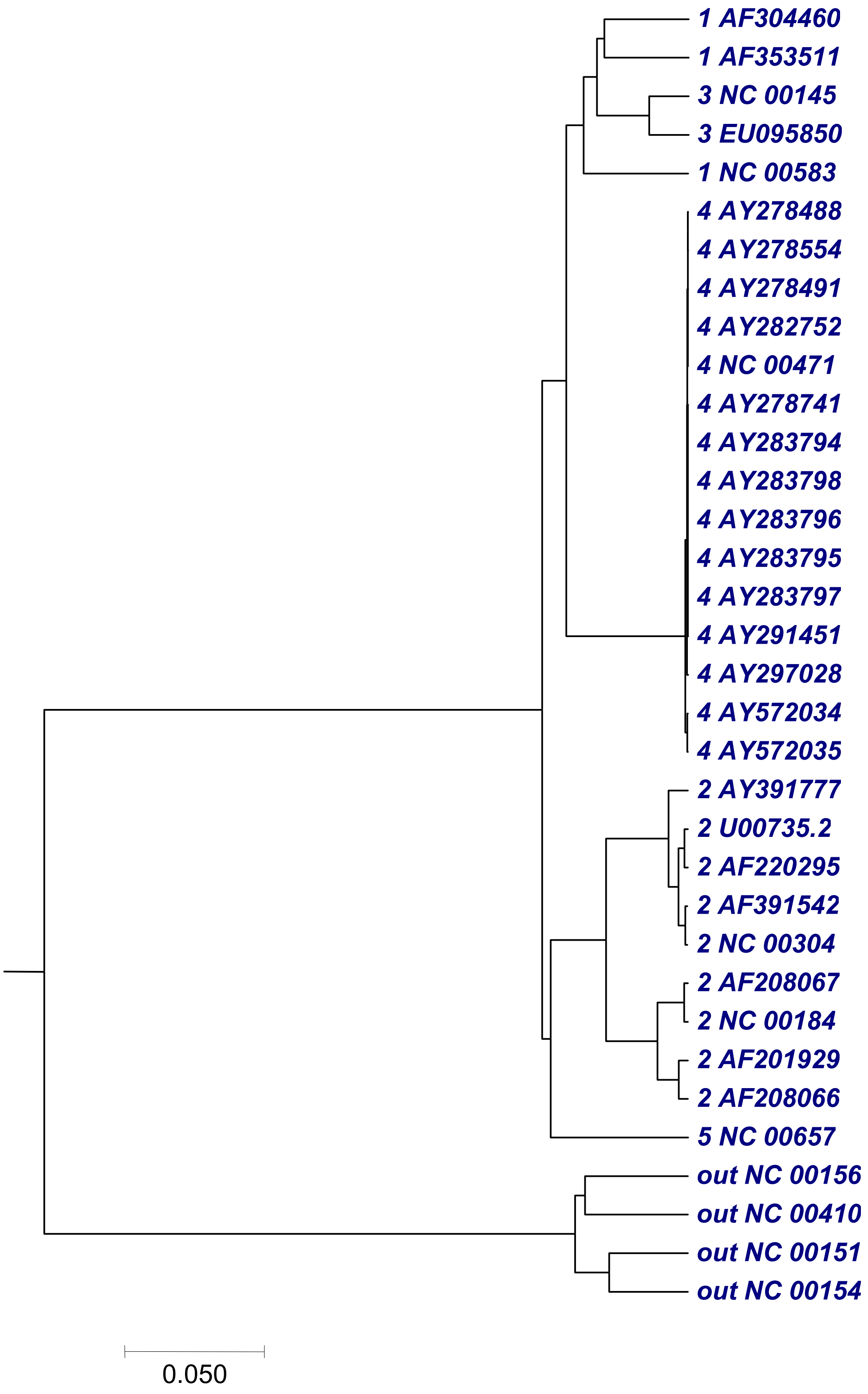

Figure 21: FFP method using string length 6.

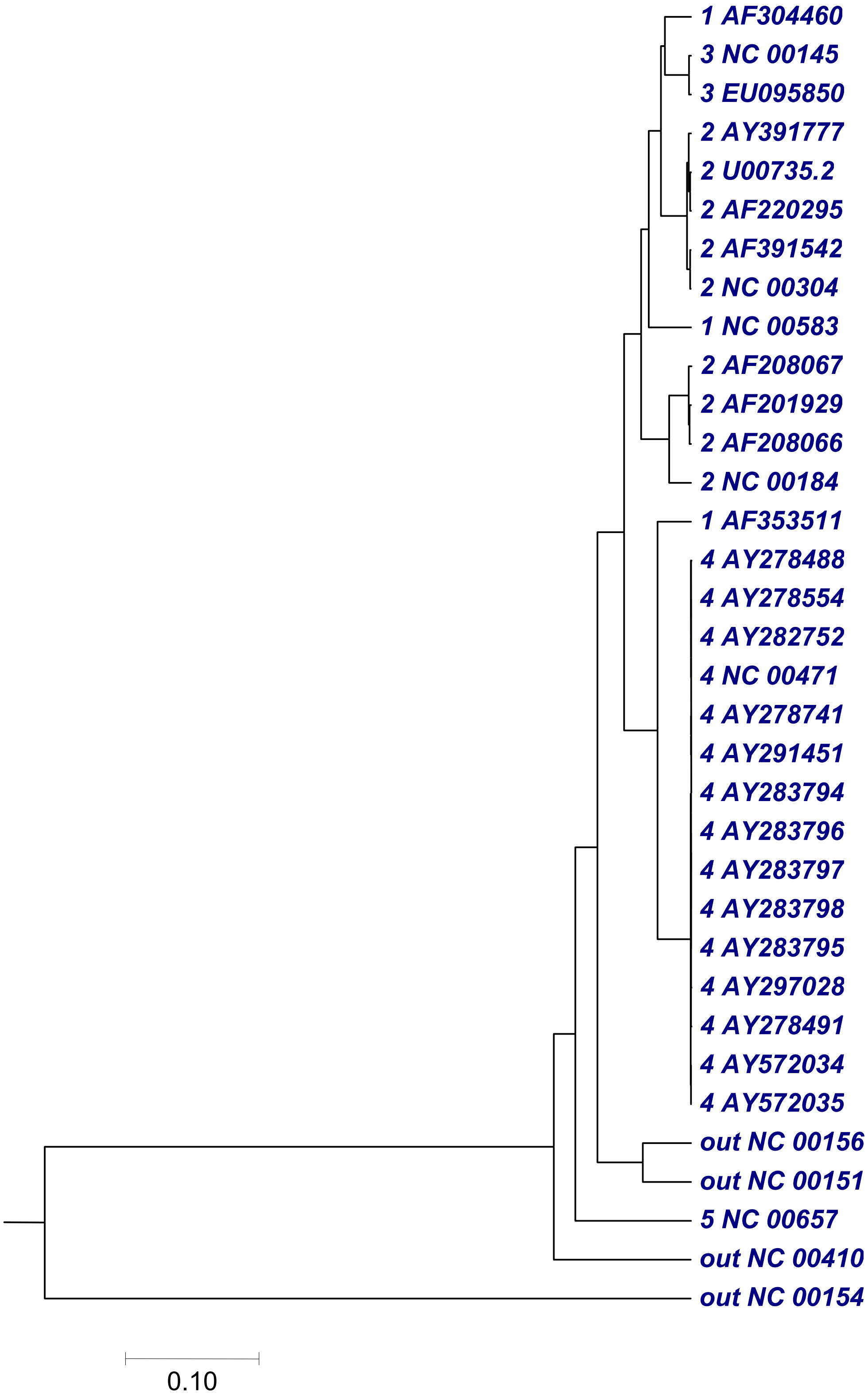

Figure 22: RTD method using string length 1.

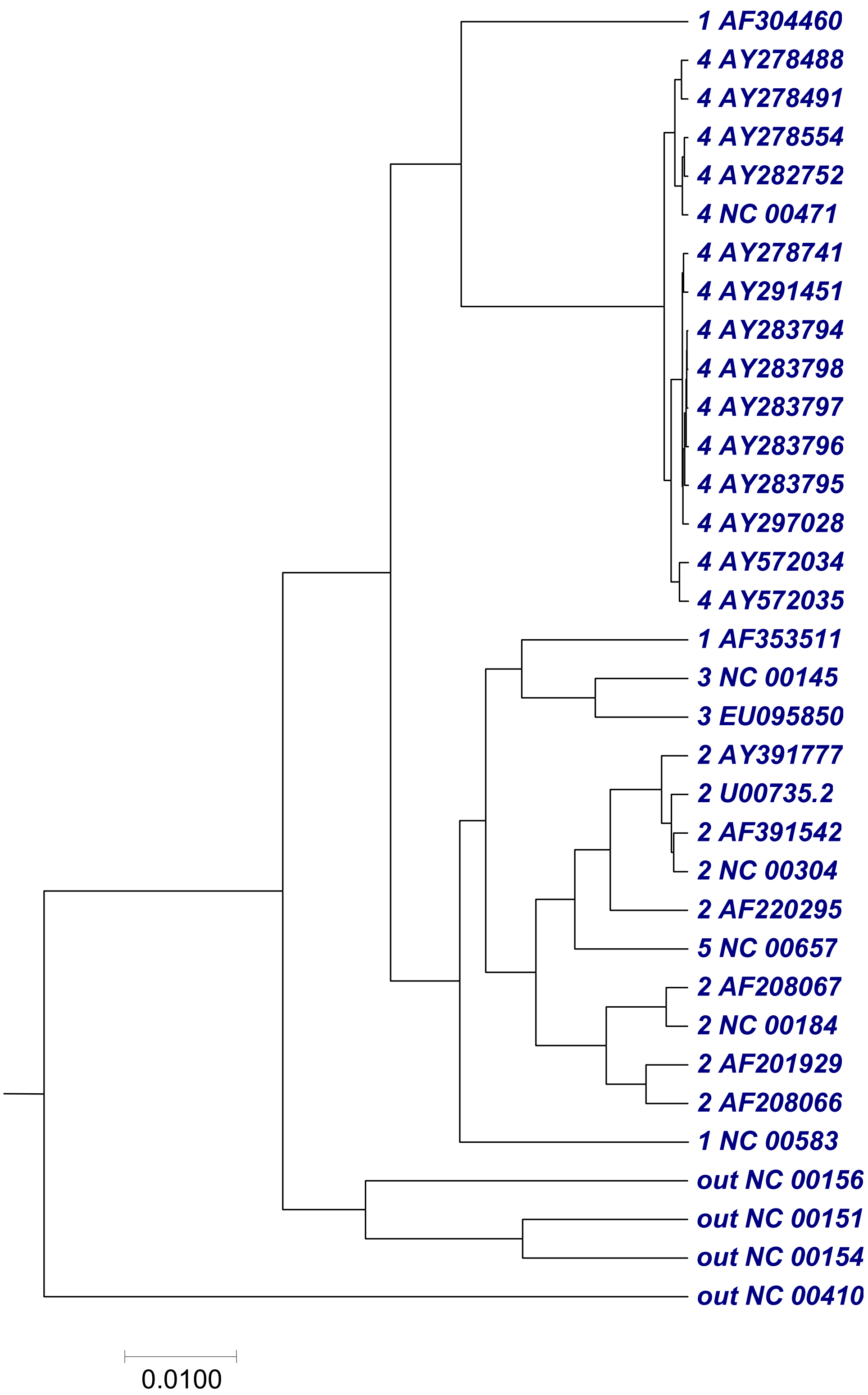

Figure 23: BBC method.

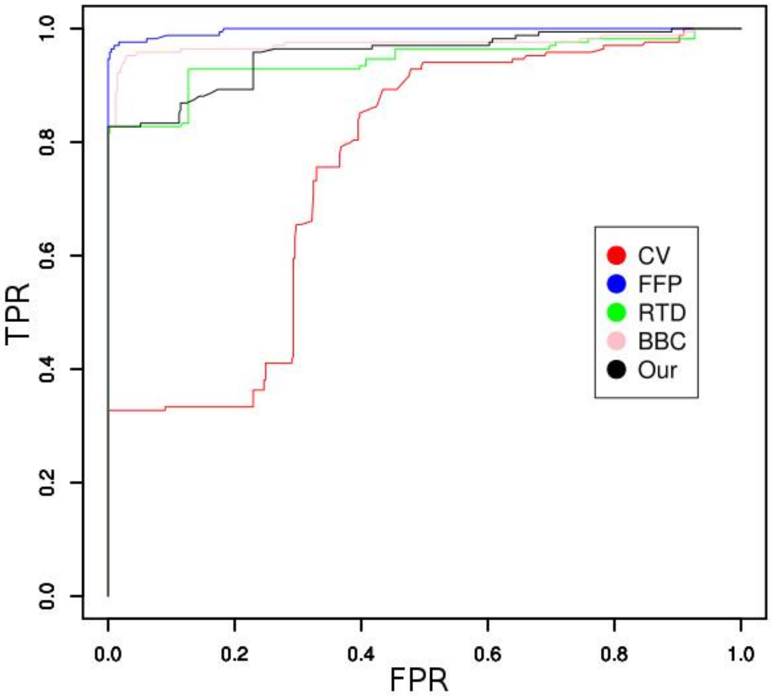

Dataset→ 30 coronavirus		
Methods↓	AUC↓	Running time↓
CV method	0.751089	1s
FFP method	0.996733	<1s
RTD method	0.942451	<1s
BBC method	0.973824	6s
Our method	0.952526	<1s

Figure 24: Receiver operating characteristic curve (ROC) and Area under the ROC Curve on 30 coronavirus sequences.

We employed our method to analyse the 30 coronavirus whole genome sequences along with 4 non-coronaviruses as outgroups. The 30 coronavirus were classified into five groups according to their host type. As shown in Figure 19 generated by our approach, we can observe that the 30 coronavirus along with 4 non-coronaviruses were correctly grouped according to their host type except group 1. We compared Figure 19 generated by our approach with Figures 20, 21, 22 and 23 prepared by other freely available tools [1]. Figure 20 did not cluster any group according to their host type. In Figures 22 and 23, the four non-coronaviruses were not clustered together. None of the methods (Figures 20, 21, 22 and 23) including our method (Figure 19) put group 1 sequences in separate clade. This shows the efficiency of our method in terms of sequence clustering. Moreover, the AUC of our method is 0.95 (Figure 24), which indicates that our method has high accuracy (Table 1).

Phylogenetic tree on 30 bacterial sequences.

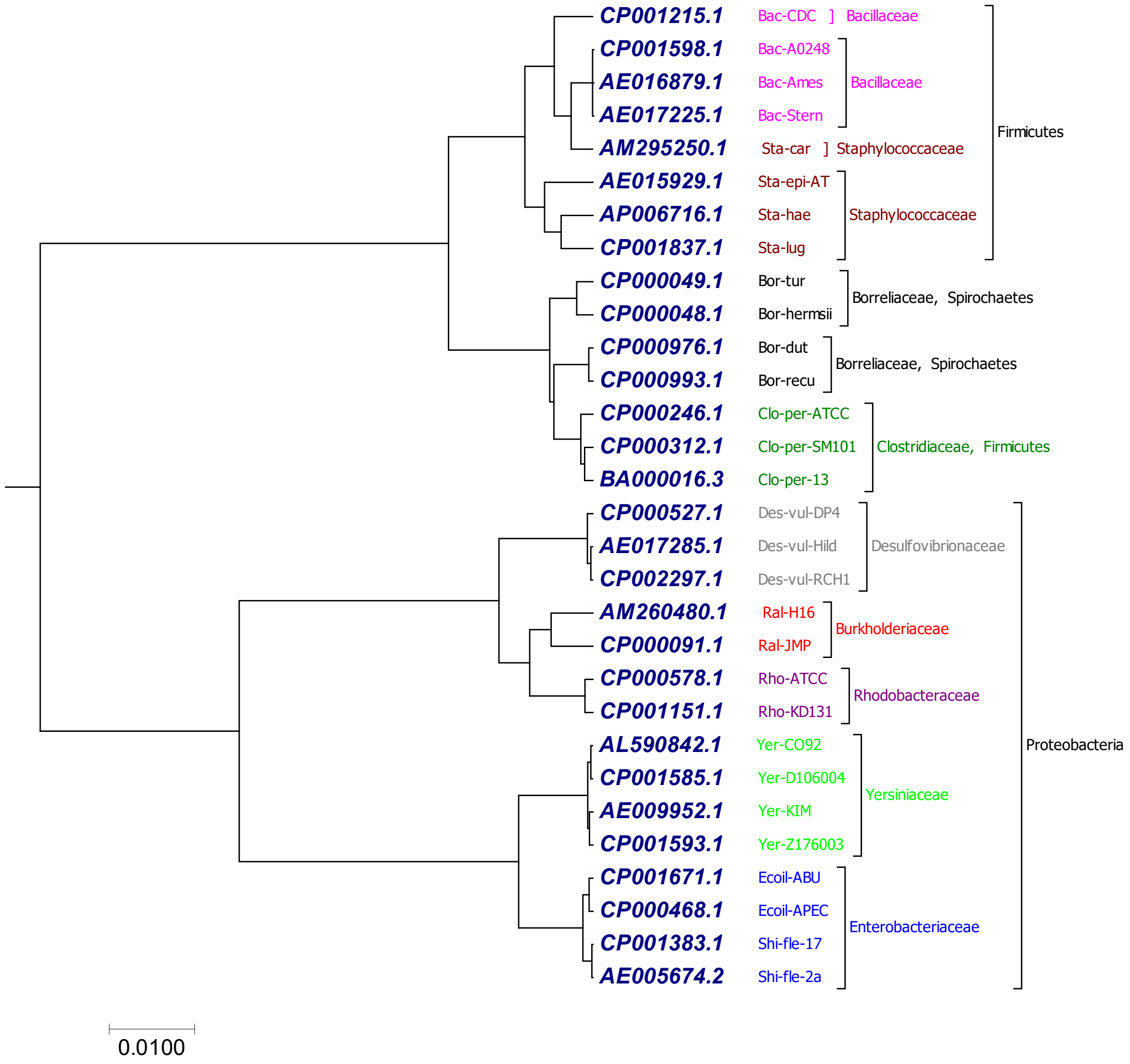

Figure 25: Our method.

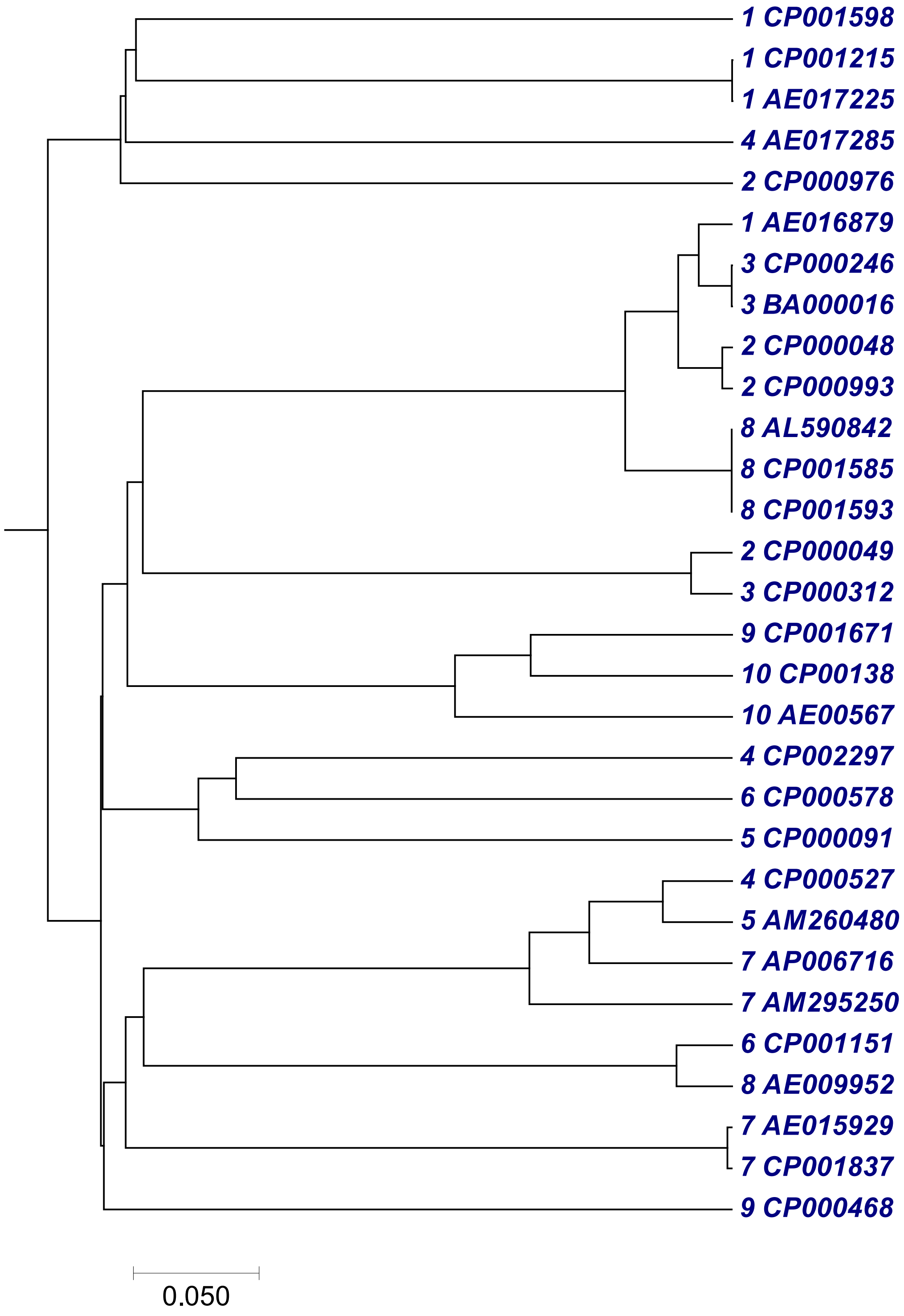

Figure 26: CV method using string length 3.

(1→Bacilleceae, 2→Borreliaceae, 3→Clostridiaceae, 4→Desulfovibrionaceae, 5→Burkholderiaceae, 6→Rhodobacteriaceae, 7→Staphylococcaceae , 8→Yersiniaceae, and 9→Enterobacteriaceae**).**

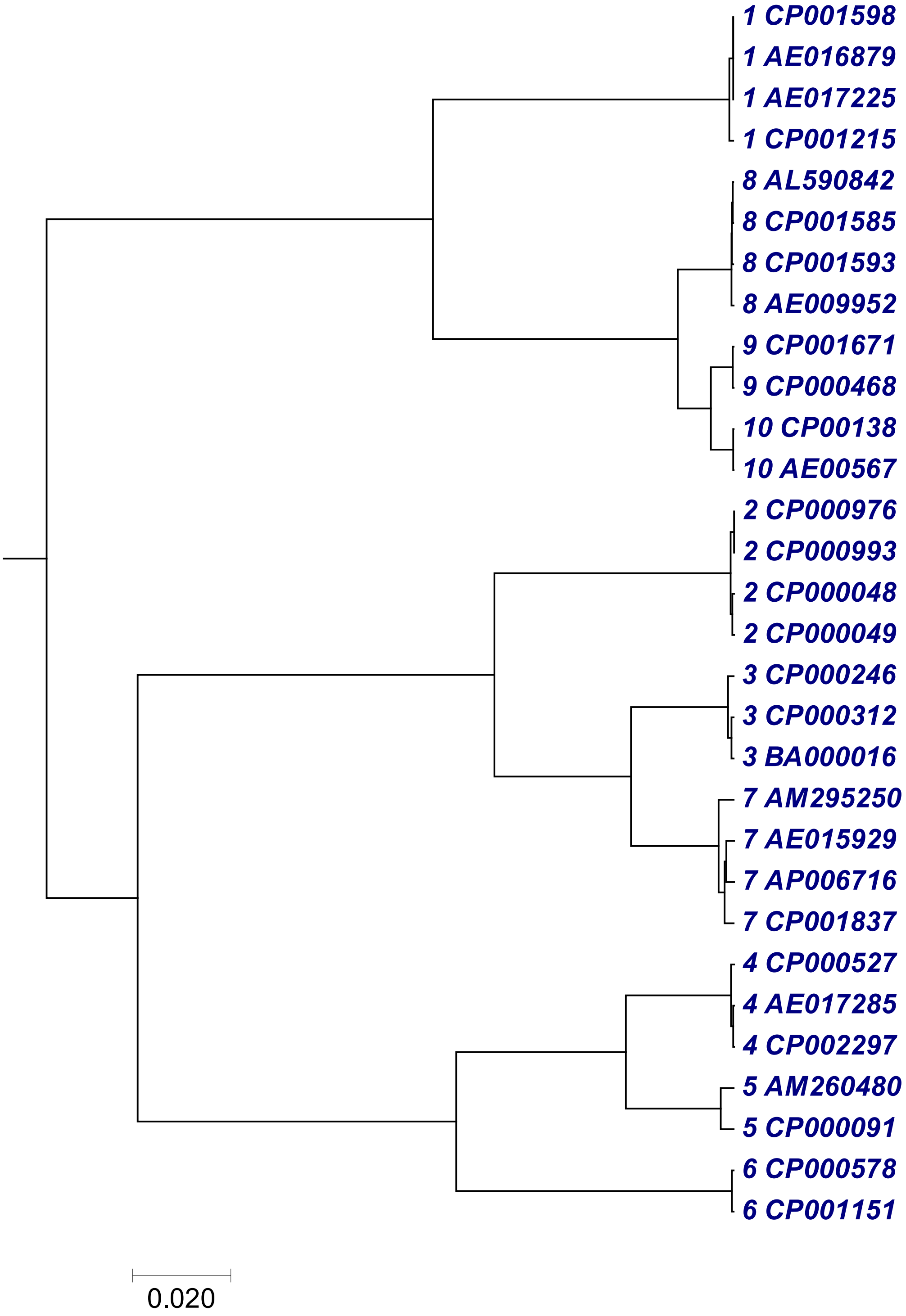

Figure 27: FFP method using string length 7.

(1→Bacilleceae, 2→Borreliaceae, 3→Clostridiaceae, 4→Desulfovibrionaceae, 5→Burkholderiaceae, 6→Rhodobacteriaceae, 7→Staphylococcaceae , 8→Yersiniaceae, and 9→Enterobacteriaceae**).**

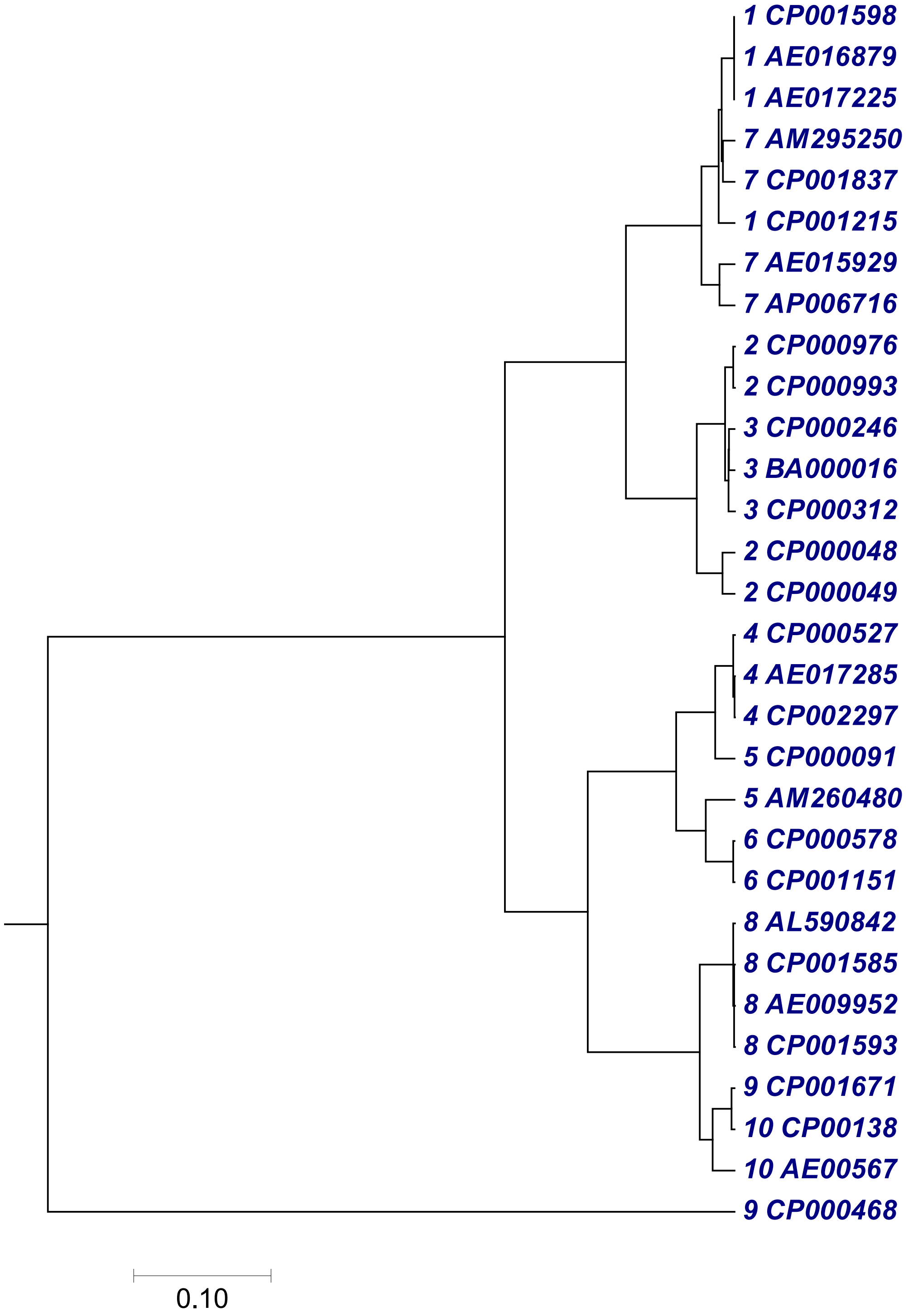

Figure 28: RTD method using string length 1.

(1→Bacilleceae, 2→Borreliaceae, 3→Clostridiaceae, 4→Desulfovibrionaceae, 5→Burkholderiaceae, 6→Rhodobacteriaceae, 7→Staphylococcaceae , 8→Yersiniaceae, and 9→Enterobacteriaceae**).**

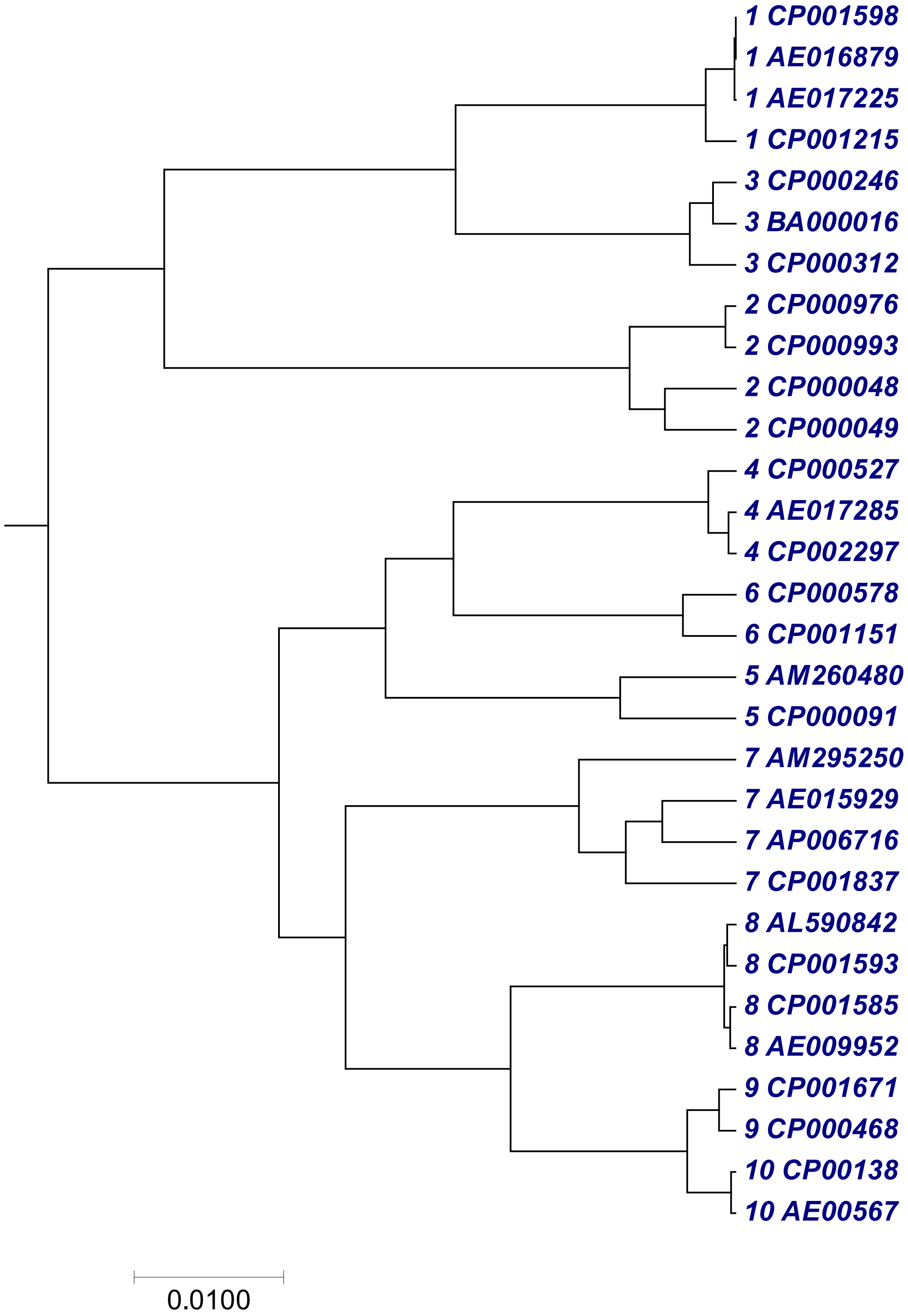

Figure 29: BBC method.

(1→Bacilleceae, 2→Borreliaceae, 3→Clostridiaceae, 4→Desulfovibrionaceae, 5→Burkholderiaceae, 6→Rhodobacteriaceae, 7→Staphylococcaceae , 8→Yersiniaceae, and 9→Enterobacteriaceae**).**

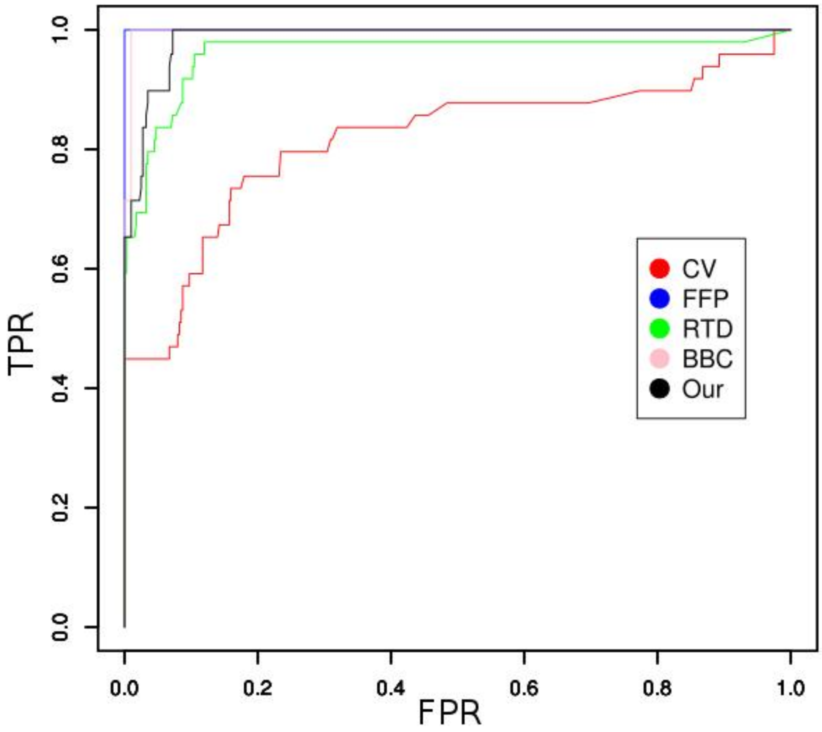

Dataset→ 30 bacterial		
Methods↓	**AUC↓**	**Running time↓**
CV method	0.814494	2m 6s
FFP method	1	1m
RTD method	0.960048	1m 14s
BBC method	0.99715	11m 33s
Our method	0.98692	3s

Figure 30: Receiver operating characteristic curve (ROC) and Area under the ROC Curve on 30 bacterial sequences.

The phylogenetic tree (Figure 25) generated by our method successfully clustered sequences based on taxnomic families such as, Burkholderiaceae, Rhodobacteriaceae, Enterobacteriaceae, Borreliaceae, Bacilleceae, Clostridiaceae, Desulfovibrionaceae, Yersiniaceae and Staphylococcaceae, which is lacking in Figures 26 and 28. However, our phylogenetic tree (Figure 25) has advantages at the phylum level over Figures 26, 27, 28 and 29. Our method (Figure 25) successfully clustered phylum Proteobacteria in a separate clade which were lacking in Figures 26, 27, 28 and 29. Moreover, the AUC of our method is 0.99 (Figure 30), which indicates that our method has high accuracy (Table 1).

Phylogenetic tree on 48 HEV sequences.

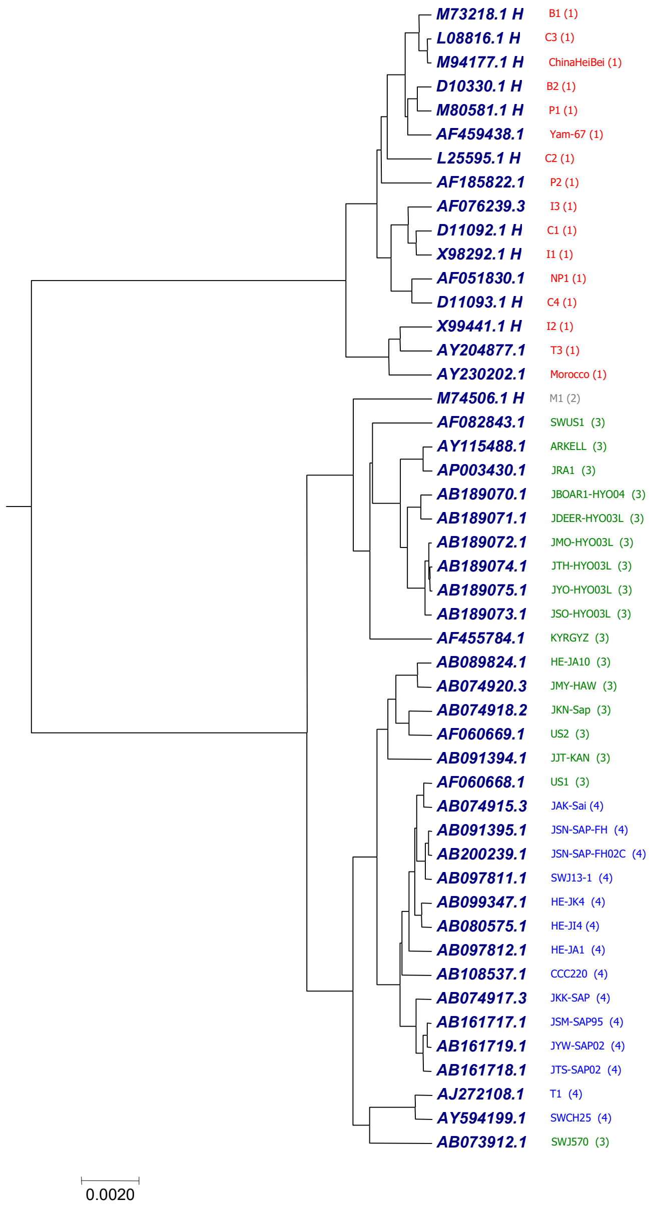

Figure 31: Our method.

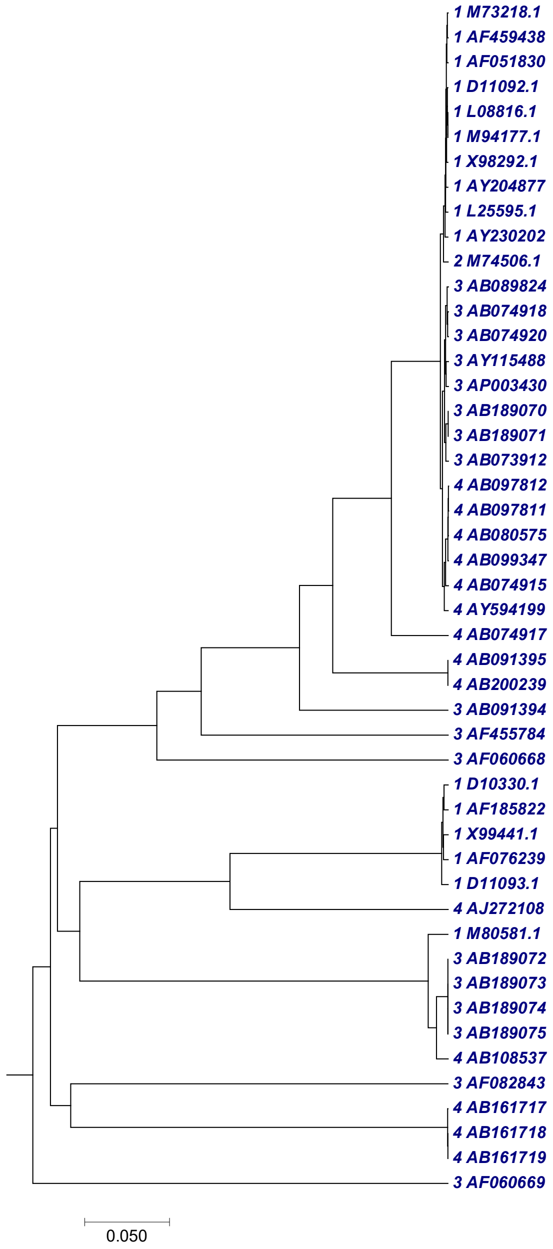

Figure 32: CV method using string length 3.

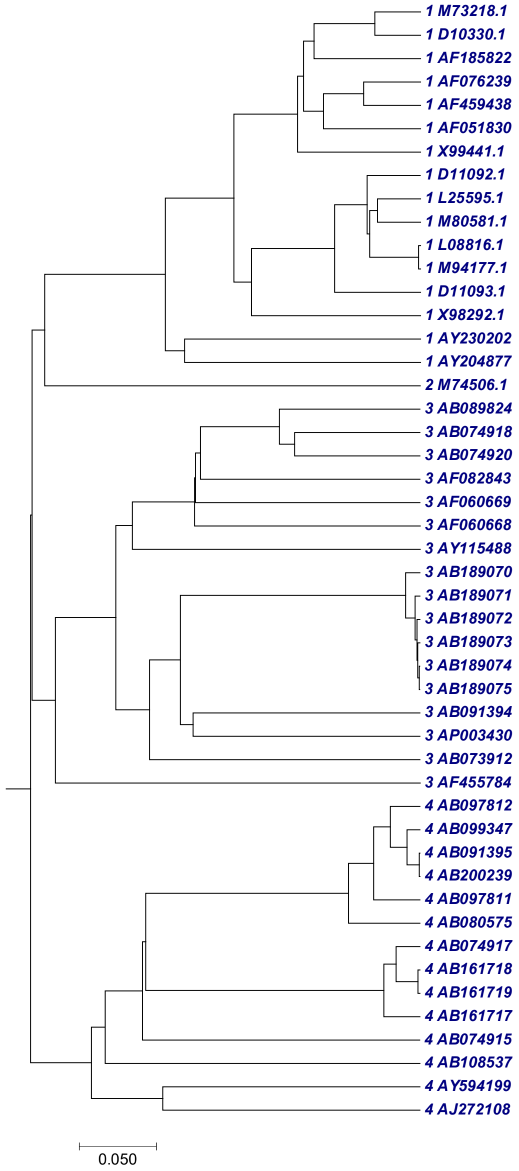

Figure 33: FFP method using string length 7.

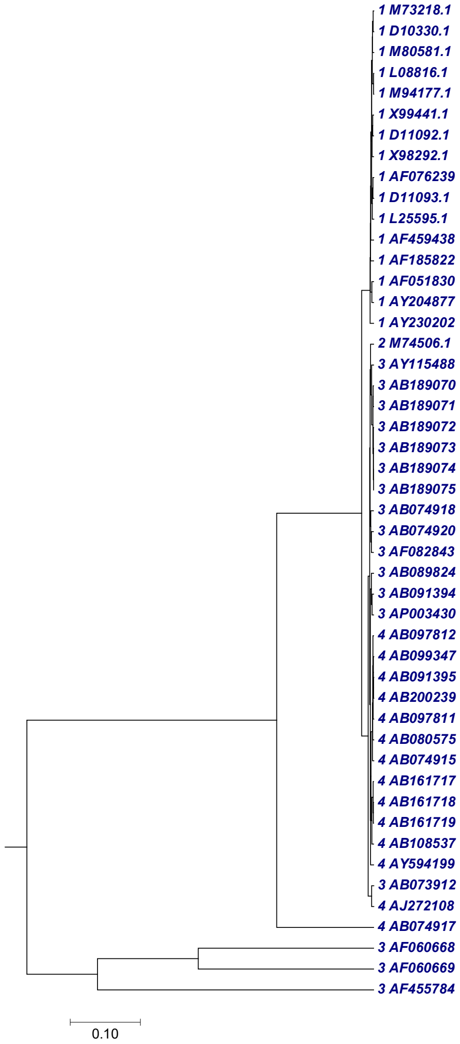

Figure 34: RTD method using string length 1.

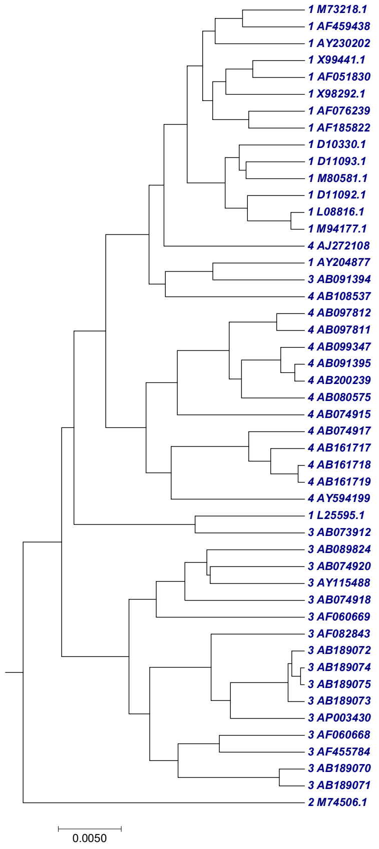

Figure 35: BBC method.

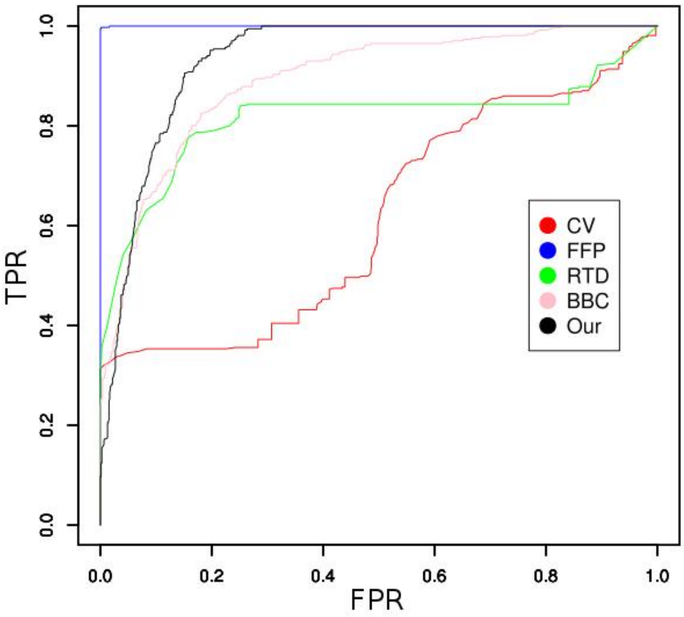

Dataset→ 48 HEV		
Methods↓	**AUC↓**	**Running time↓**
CV method	0.614583	<1s
FFP method	0.999952	1s
RTD method	0.808687	<1s
BBC method	0.891211	2s
Our method	0.933716	<1s

Figure 36: Receiver operating characteristic curve (ROC) and Area under the ROC Curve on 48 HEV sequences.

As shown in Figure 31 generated by our approach, the HEV genomes were divided into separate clades based on four genotypic categories (1(red),2(grey), 3(green) and 4(blue)) except few sequences. We compared the phylogenetic tree (Figure 31) generated by our approach with the phylogenetic trees (Figures 32, 33, 34 and 35) prepared by other freely available tools [1]. In Figure 32, four genotypic classes were not properly clustered. In Figures 34 and 35, four genotypic categories were separately clustered except few sequences. In Figure 33, all HEV genomes were correctly divided into separate clades based on four genotypic categories. Above performance shows the advantage of our method over other methods (Figures 32, 34 and 35) in terms of sequence clustering. Moreover, the AUC of our method is 0.93 (Figure 36), which indicates that our method has high accuracy (Table 1).

Phylogenetic tree on 58 mixed sequences.

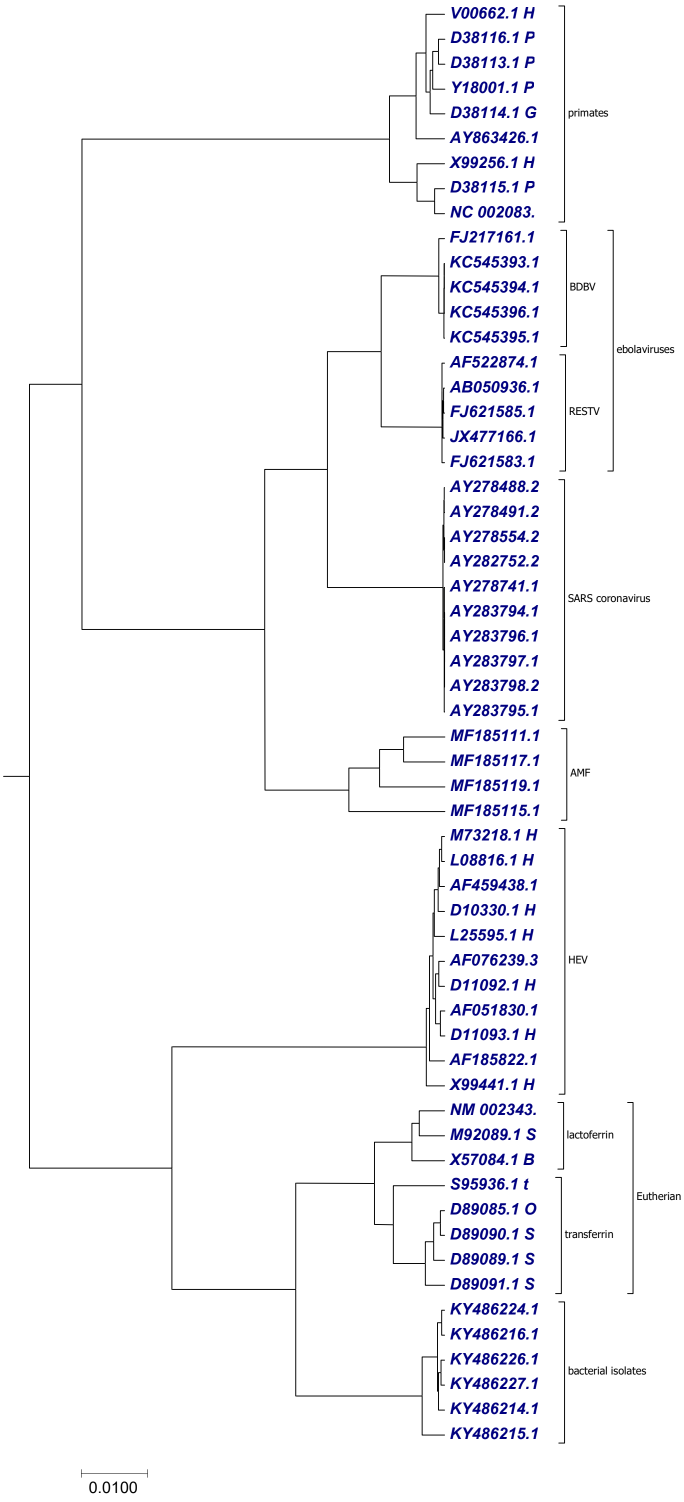

Figure 37: Our method.

(1→ primates, 2 → ebolavirus, 3→ SARS coronavirus, 4→ HEV, 5→ eutherian, 6 →AMF and 7→ bacterial isolates.)

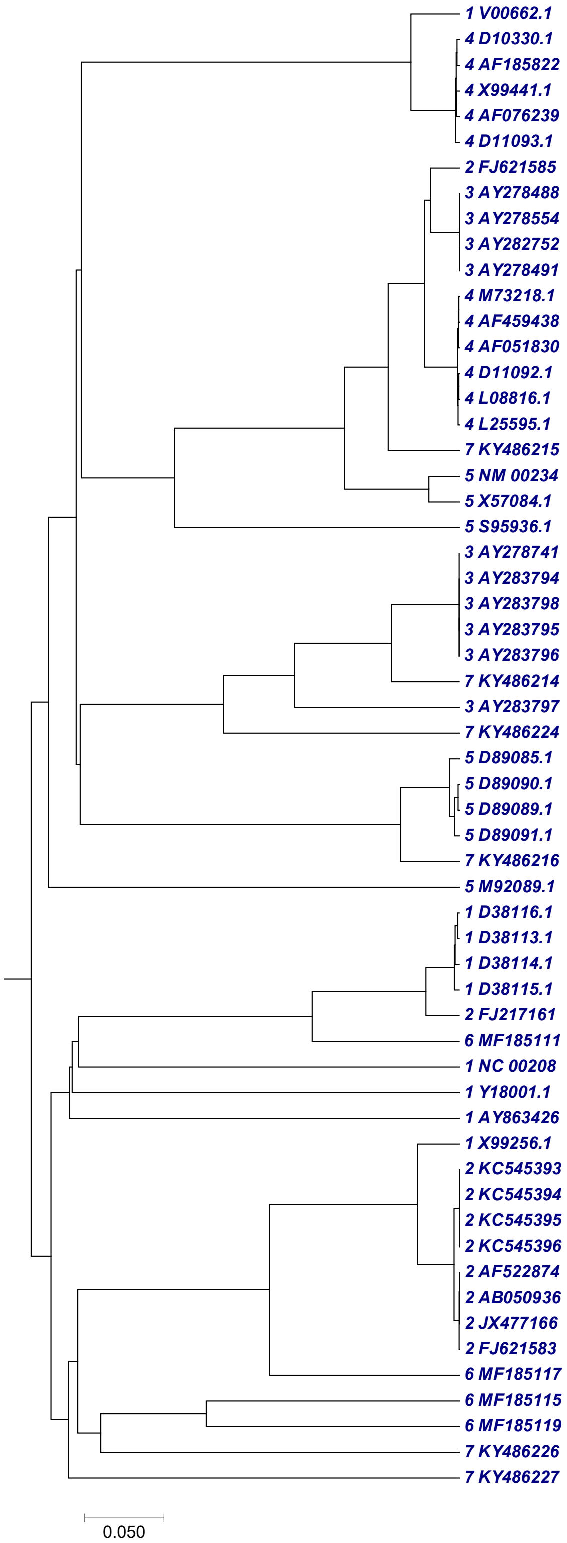

Figure 38: CV method using string length 3.

(1→ primates, 2 → ebolavirus, 3→ SARS coronavirus, 4→ HEV, 5→ eutherian, 6 →AMF and 7→ bacterial isolates.)

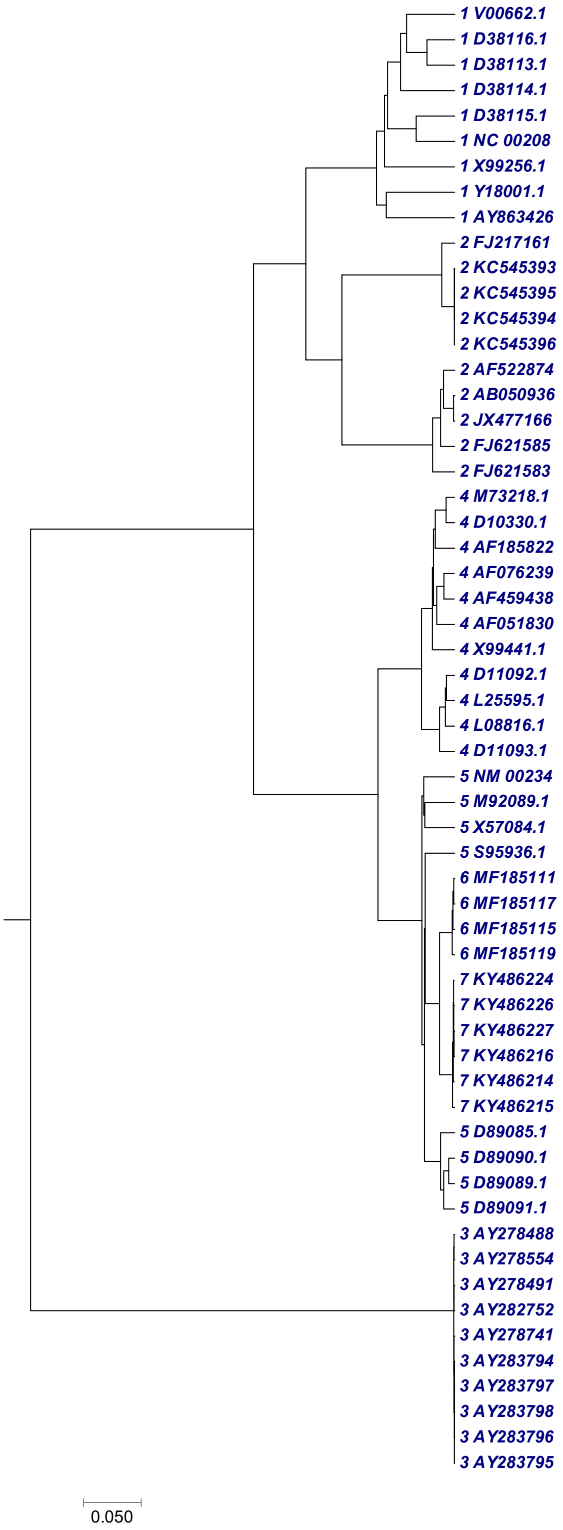

Figure 39: FFP method using string length 7.

(1→ primates, 2 → ebolavirus, 3→ SARS coronavirus, 4→ HEV, 5→ eutherian, 6 →AMF and 7→ bacterial isolates.)

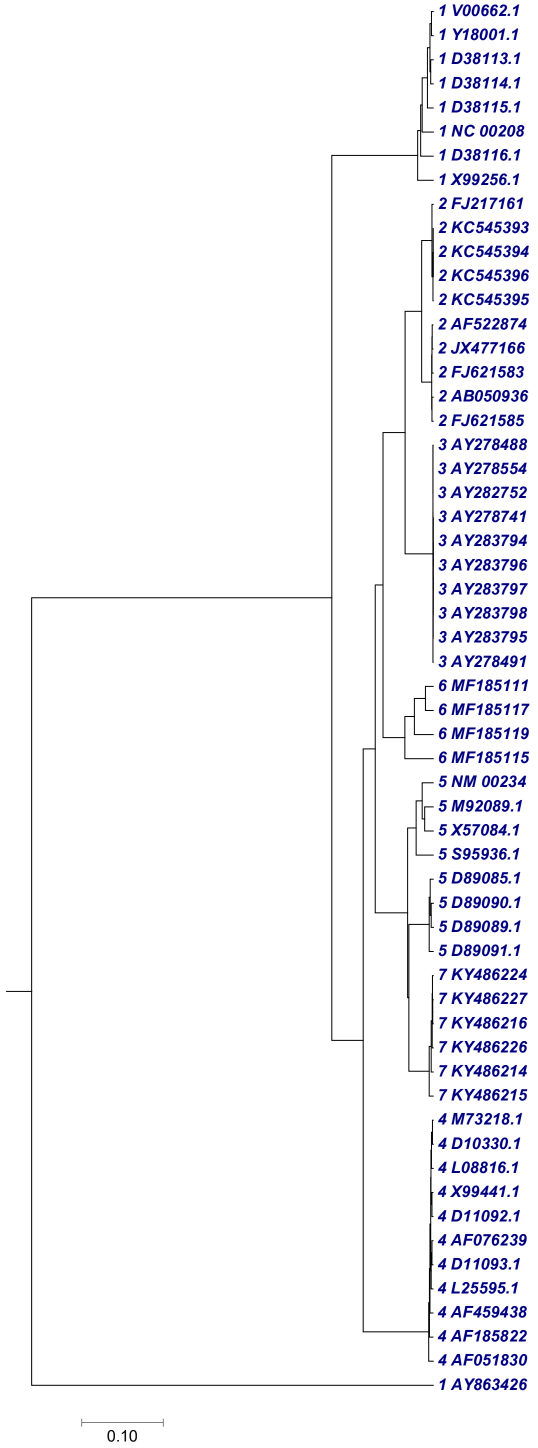

Figure 40: RTD method using string length 1.

(1→ primates, 2 → ebolavirus, 3→ SARS coronavirus, 4→ HEV, 5→ eutherian, 6 →AMF and 7→ bacterial isolates.)

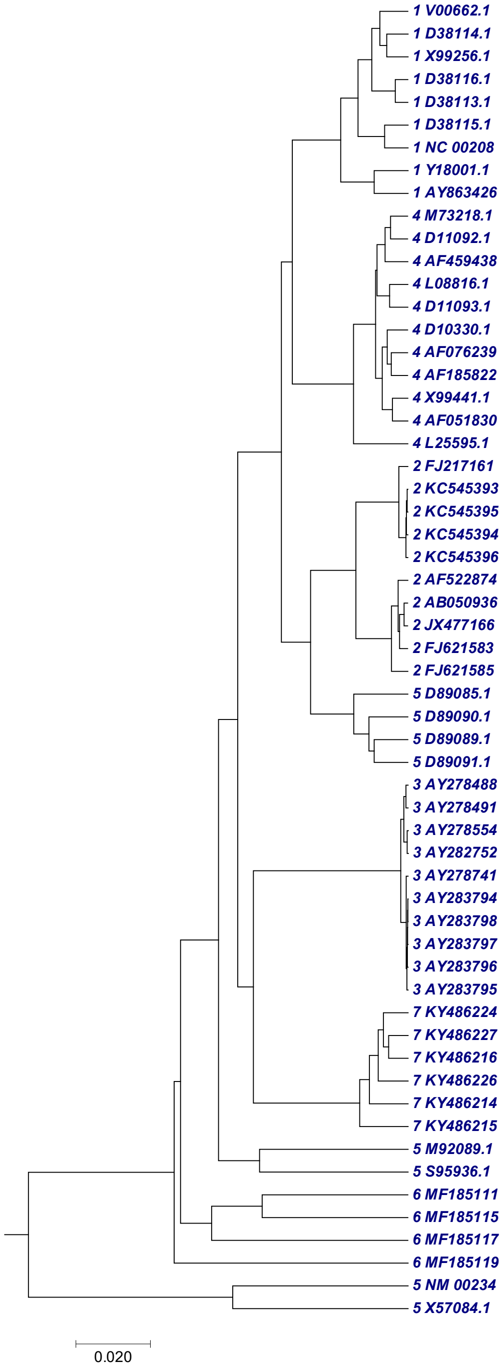

Figure 41: BBC method.

(1→ primates, 2 → ebolavirus, 3→ SARS coronavirus, 4→ HEV, 5→ eutherian, 6 →AMF and 7→ bacterial isolates.)

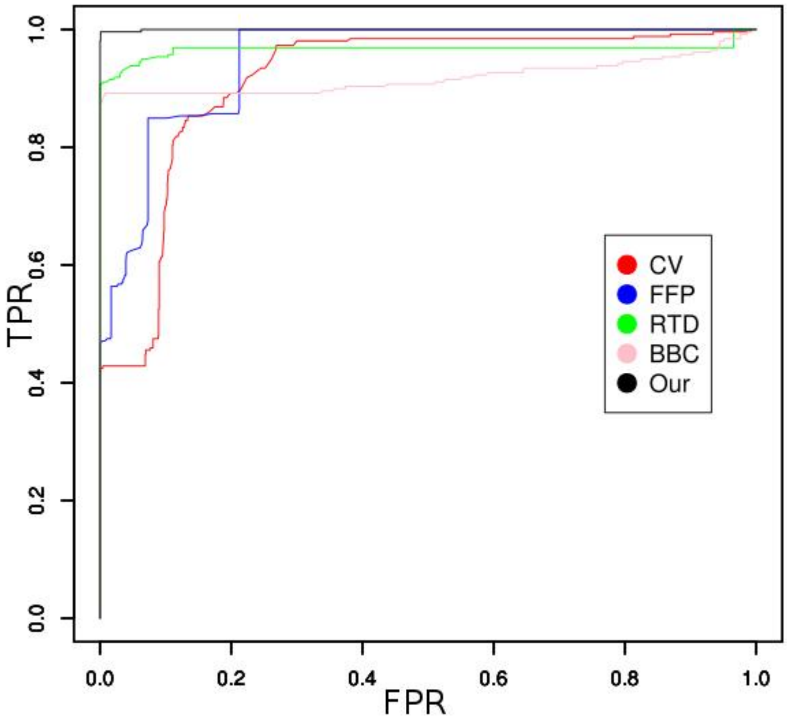

Dataset→ 58 mixed		
Methods↓	**AUC↓**	**Running time↓**
CV method	0.91396	1s
FFP method	0.948556	2s
RTD method	0.966549	<1s
BBC method	0.918997	5s
Our method	0.999748	<1s

Figure 42: Receiver operating characteristic curve (ROC) and Area under the ROC Curve on 58 mixed sequences.

We collected 58 genome dataset from different species, which includes nine primates mammalian mitochondrial genomes, ten ebolavirus (five reston virus (RESTV), five bundibugyo virus (BDBV)) complete genomes, ten SARS coronavirus, eleven hepatitis E virus, eight eutherian mammal, four arbuscular mycorrhizal fungi and six bacterial isolates. As shown in Figure 37 generated by our method, we observed that all the different species genome datasets were clustered separately. We compared the phylogenetic tree (Figure 37) generated by our approach with the phylogenetic trees (Figures 38, 39, 40 and 41) prepared by other freely available tools [1]. In Figure 38, 58 genome datasets from different species were not properly clustered. In Figures 39, 40 and 41, eight eutherian mammals were divided into more than one clades. . In addition to the superior phylogenetic tree, the AUC of our method is 0.99 (Figure 42), which indicates that our method has high accuracy (Table 1).

Phylogenetic tree on 29 escherichia/shigella sequences.

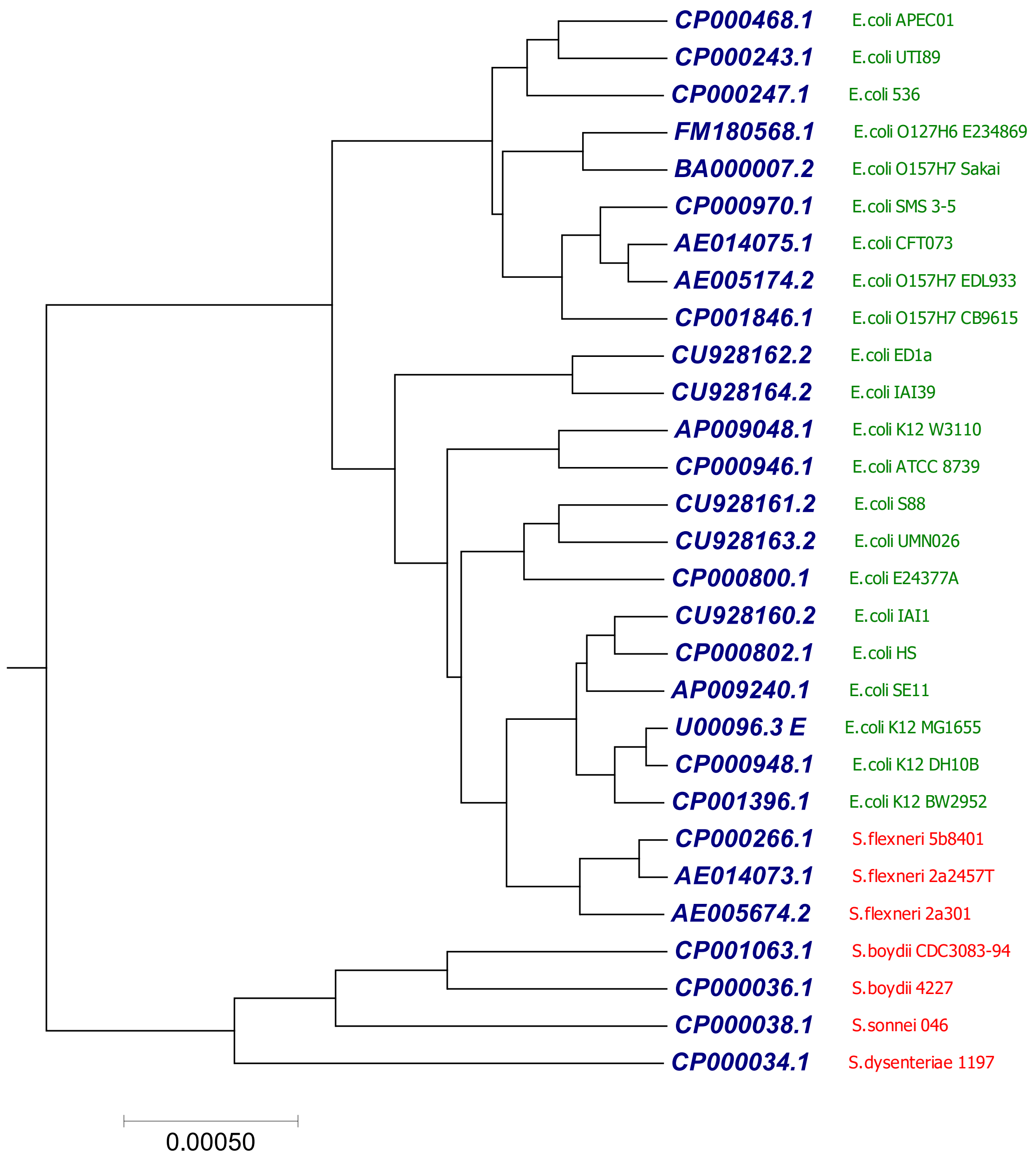
CP000468.1 E.coli APEC01
CP000243.1 E.coli UTI89
CP000247.1 E.coli 536
FM180568.1 E.coli O127H6 E234869
BA000007.2 E.coli O157H7 Sakai
CP000970.1 E.coli SMS 3-5
AE014075.1 E.coli CFT073
AE005174.2 E.coli O157H7 EDL933
CP001846.1 E.coli O157H7 CB9615
CU928162.2 E.coli ED1a
CU928164.2 E.coli IAI39
AP009048.1 E.coli K12 W3110
CP000946.1 E.coli ATCC 8739
CU928161.2 E.coli S88
CU928163.2 E.coli UMN026
CP000800.1 E.coli E24377A
CU928160.2 E.coli IAI1
CP000802.1 E.coli HS
AP009240.1 E.coli SE11
U00096.3 E E.coli K12 MG1655
CP000948.1 E.coli K12 DH10B
CP001396.1 E.coli K12 BW2952
CP000266.1 S.flexneri 5b8401
AE014073.1 S.flexneri 2a2457T
AE005674.2 S.flexneri 2a301
CP001063.1 S.boydii CDC3083-94
CP000036.1 S.boydii 4227
CP000038.1 S.sonnei 046
CP000034.1 S.dysenteriae 1197
0.00050

Figure 43: Our method.

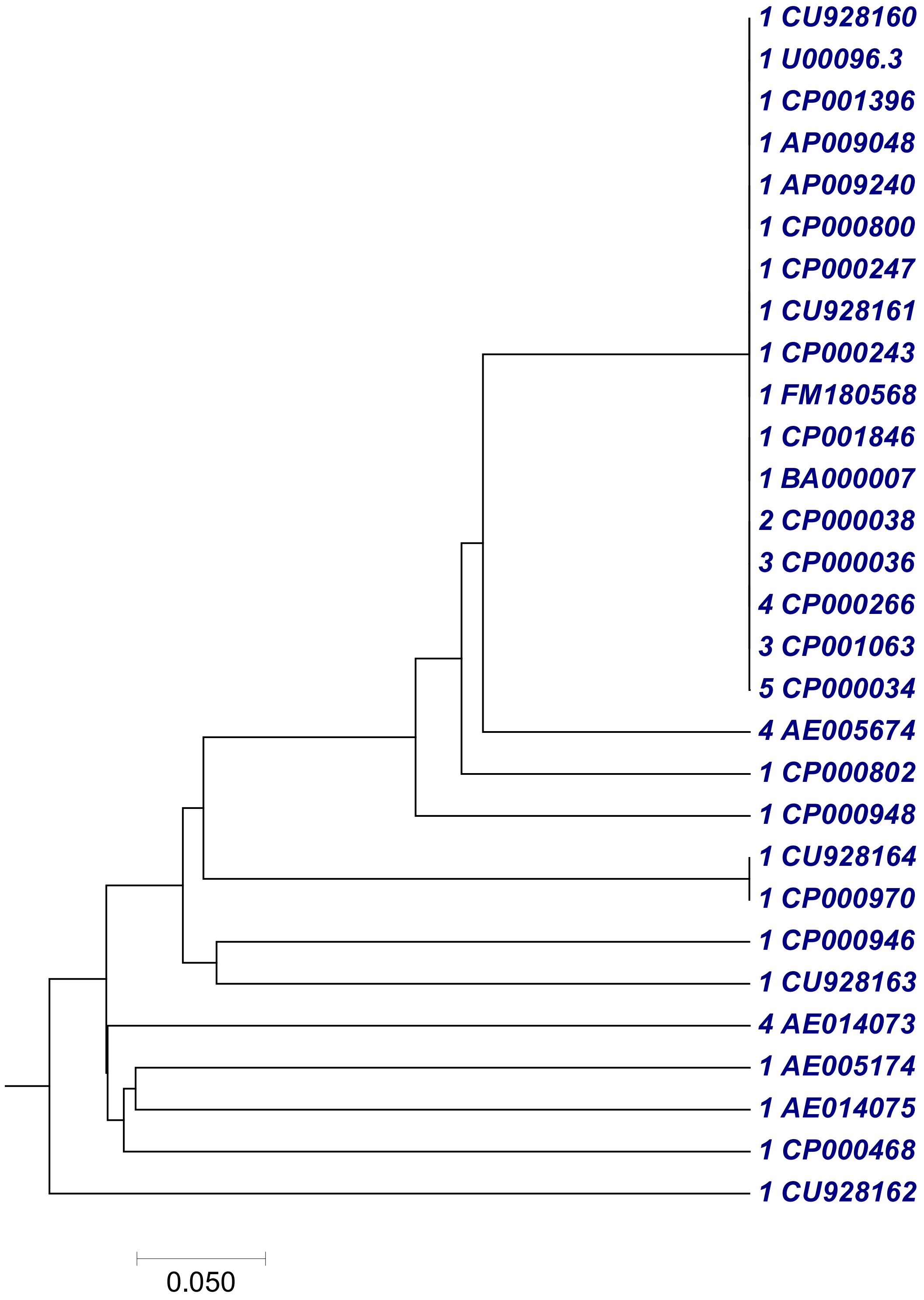

Figure 44: CV method using string length 3.

(1→ E.coli, 4→S.flexneri, 3→S.boydii, 2→S.sonnei and 5→S.dysenteriae).

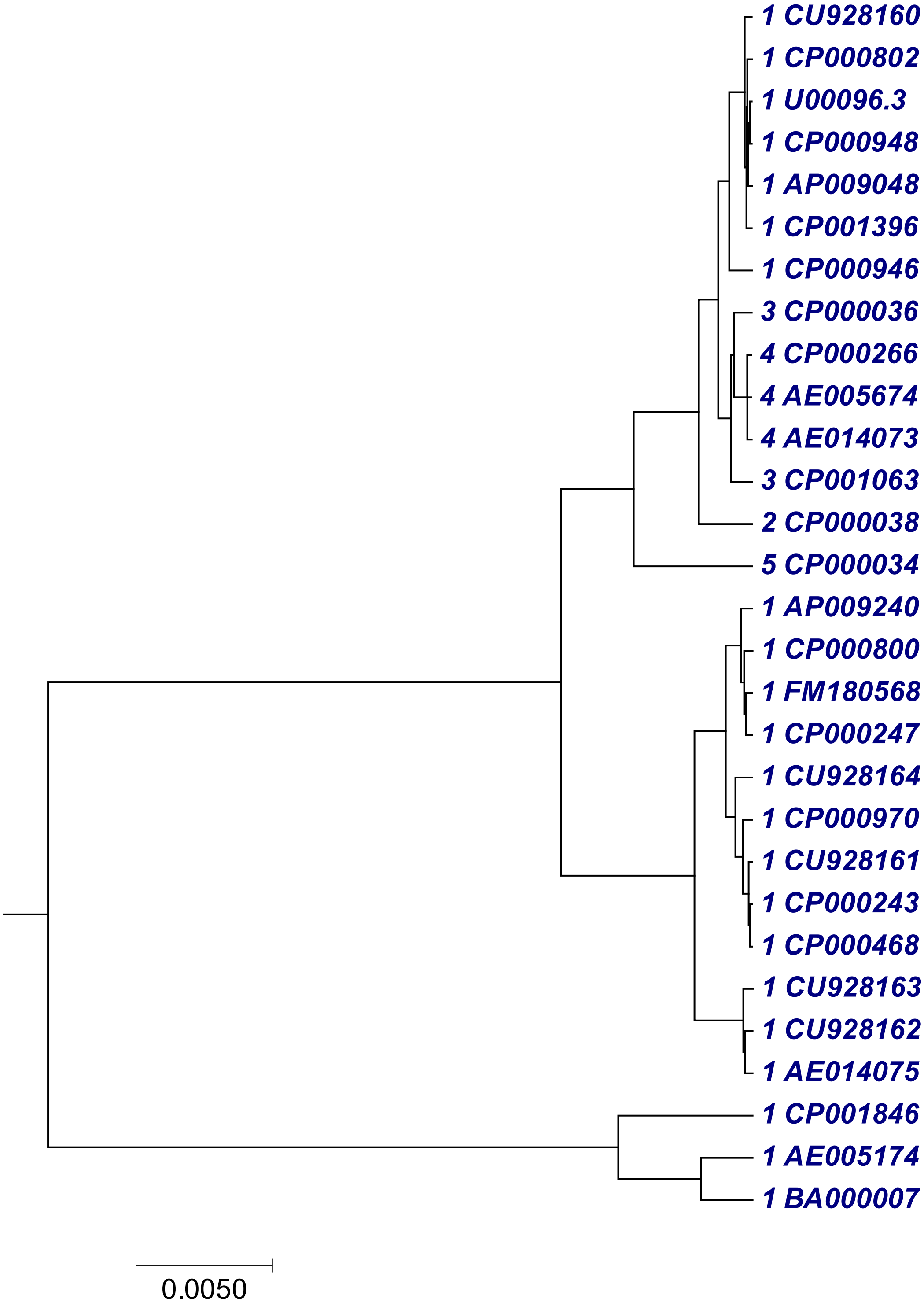

Figure 45: FFP method using string length 7.

(1→ E.coli, 4→S.flexneri, 3→S.boydii, 2→S.sonnei and 5→S.dysenteriae).

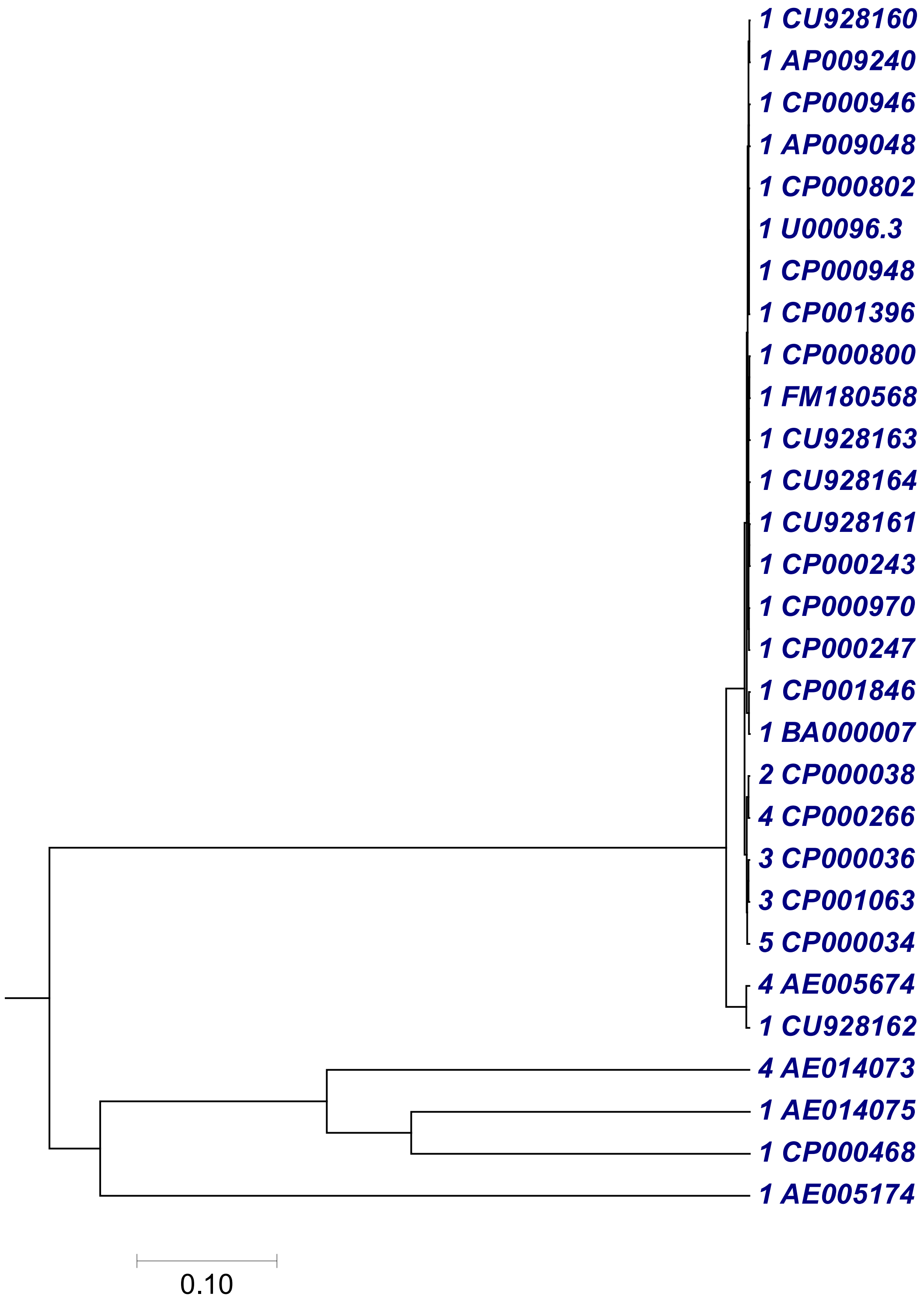

Figure 46: RTD method using string length 1.

(1→ E.coli, 4→S.flexneri, 3→S.boydii, 2→S.sonnei and 5→S.dysenteriae).

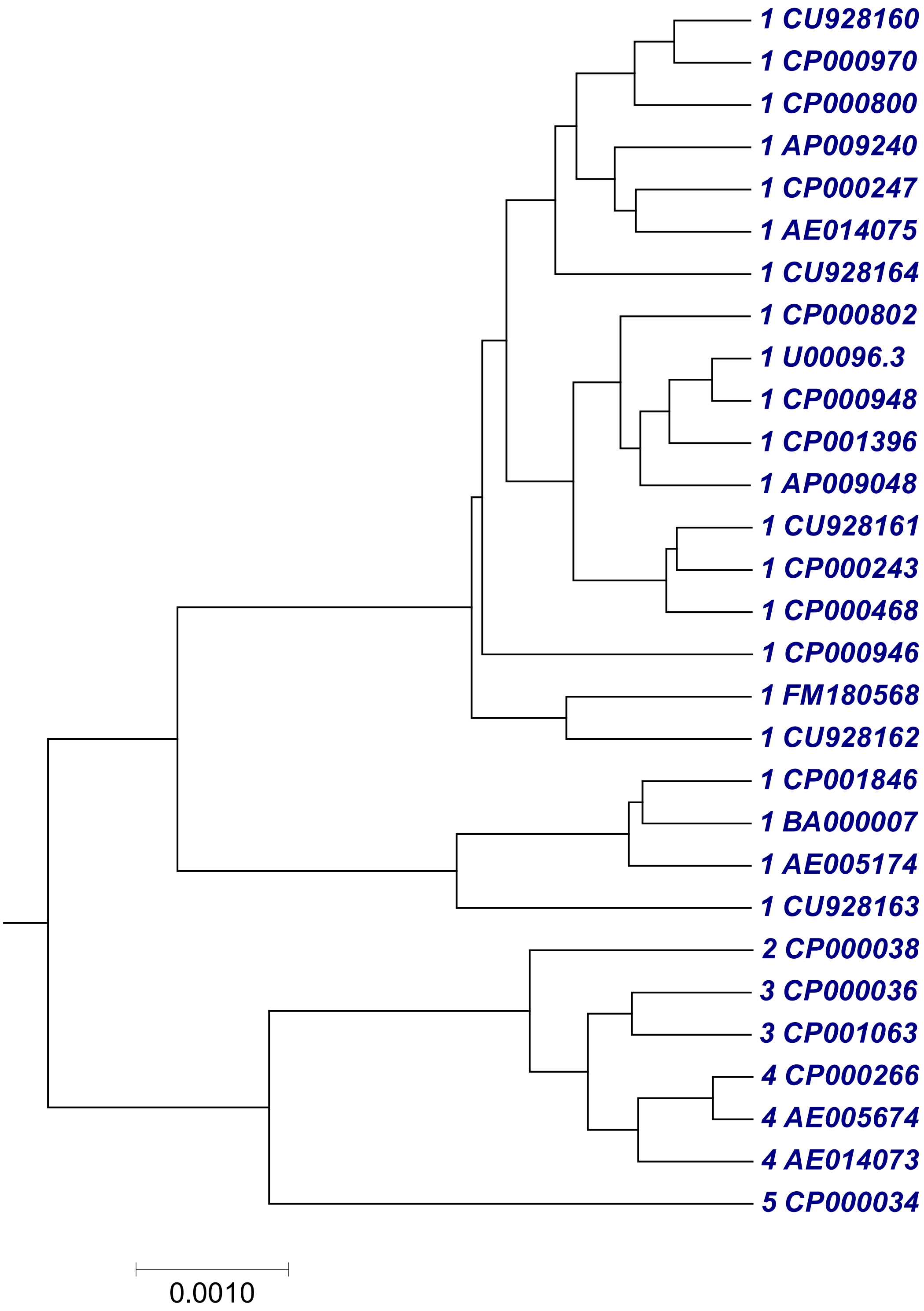

Figure 47: BBC method.

(1→ E.coli, 4→S.flexneri, 3→S.boydii, 2→S.sonnei and 5→S.dysenteriae).

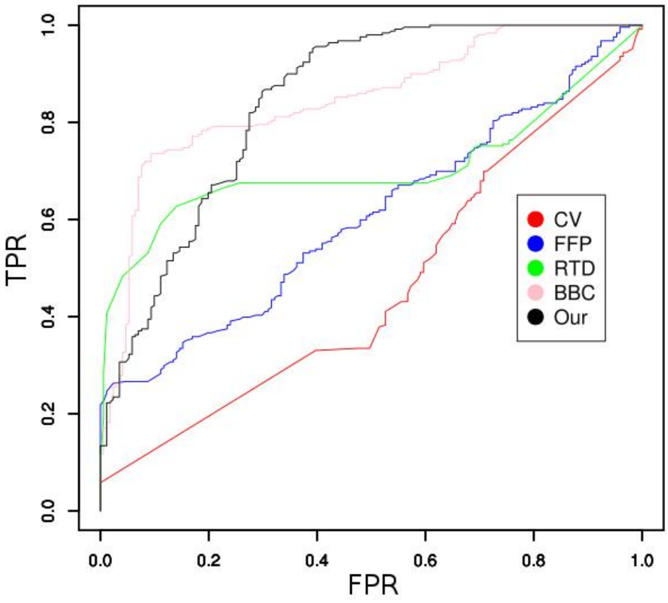

Dataset→	29 Escherichia/ Shigella	
Methods↓	**AUC↓**	**Running time↓**
CV method	0.377468	1m 45s
FFP method	0.60405	1m 2s
RTD method	0.671132	1m 6s
BBC method	0.84575	16m 52s
Our method	0.842633	3s

Figure 48: Receiver operating characteristic curve (ROC) and Area under the ROC Curve on 29 Escherichia/Shigella sequences.

The phylogenetic tree (Figure 43) generated by our method successfully clustered all organisms belongs to Escherichia coli, Shigella flexneri and Shigella boydii in separate clades. While comparing the tree prepared by our method (Figure 43) with the tree prepared by other freely available tools [1] (Figures 44, 45, 46 and 47). We found that, all organisms belong to Escherichia coli were not properly clustered in Figures 44, 45 and 46. However, Figure 47 has similarity with our result. However, the AUC of our method is 0.84 (Figure 48), which indicates that our method has moderate accuracy (Table 1).

Phylogenetic tree on 24 eutherian sequences.

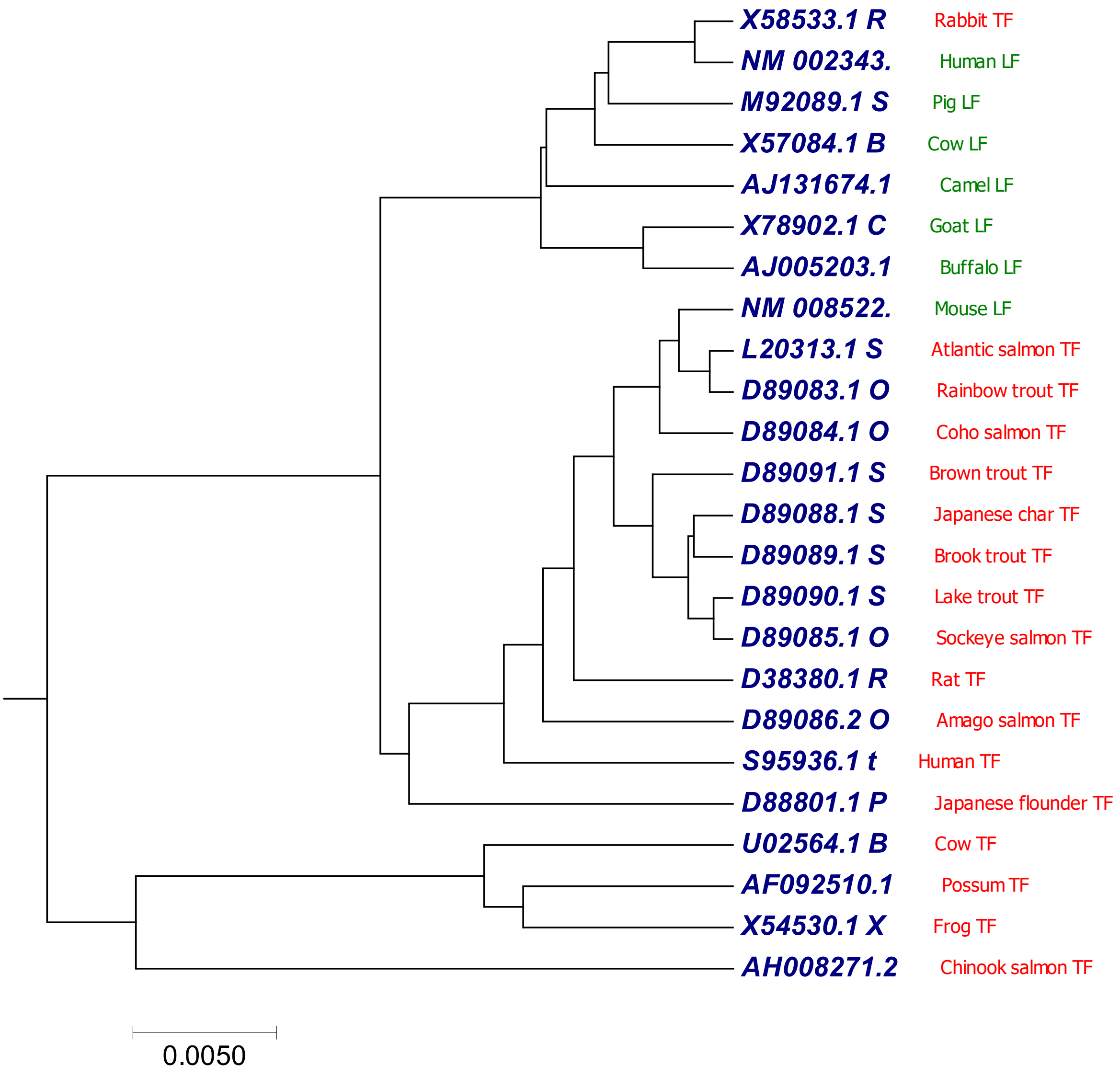
X58533.1 R Rabbit TF
NM 002343. Human LF
M92089.1 S Pig LF
X57084.1 B Cow LF
AJ131674.1 Camel LF
X78902.1 C Goat LF
AJ005203.1 Buffalo LF
NM 008522. Mouse LF
L20313.1 S Atlantic salmon TF
D89083.1 O Rainbow trout TF
D89084.1 O Coho salmon TF
D89091.1 S Brown trout TF
D89088.1 S Japanese char TF
D89089.1 S Brook trout TF
D89090.1 S Lake trout TF
D89085.1 O Sockeye salmon TF
D38380.1 R Rat TF
D89086.2 O Amago salmon TF
S95936.1 t Human TF
D88801.1 P Japanese flounder TF
U02564.1 B Cow TF
AF092510.1 Possum TF
X54530.1 X Frog TF
AH008271.2 Chinook salmon TF
0.0050

Figure 49: Our method.

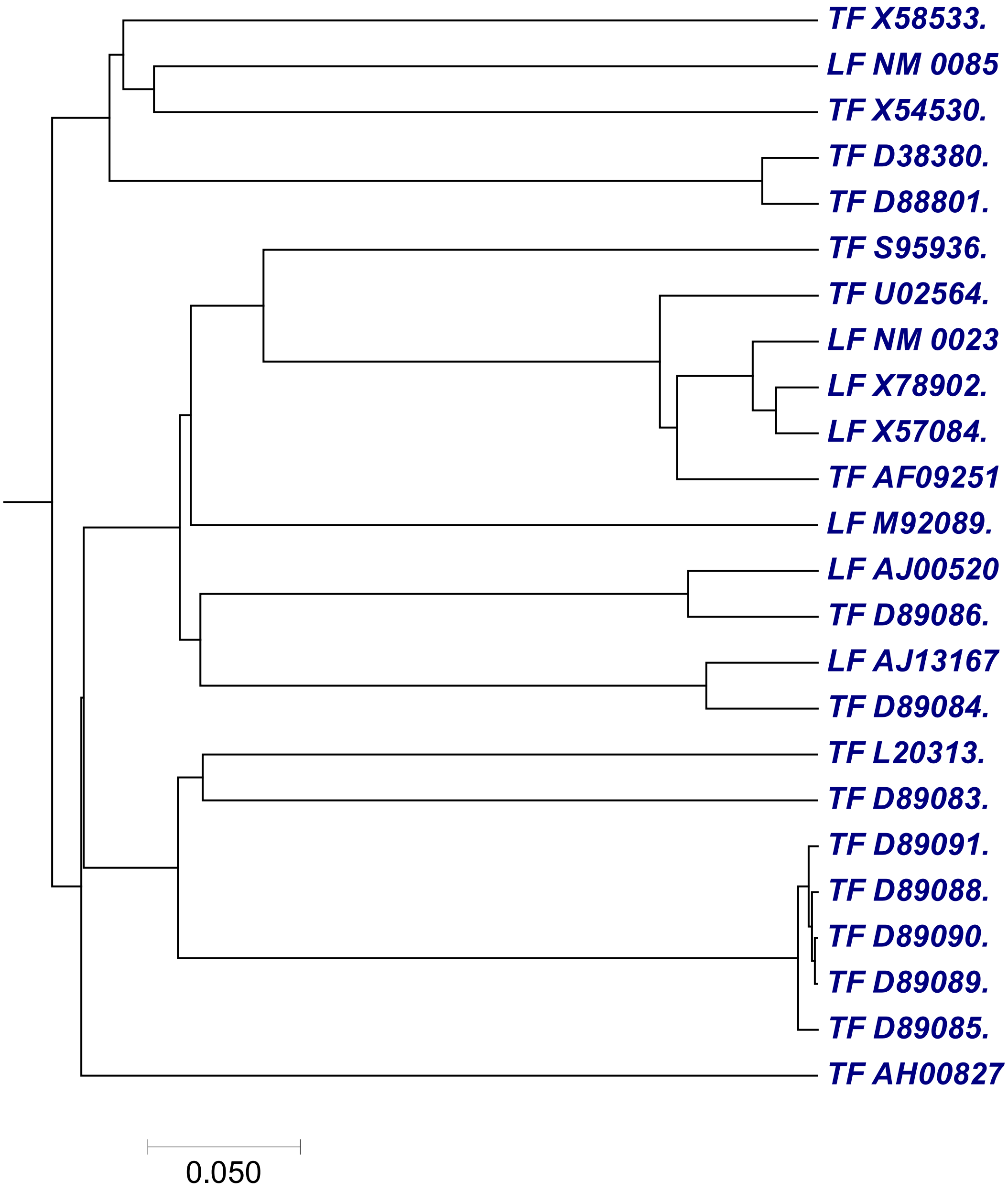

Figure 50: CV method using string length 3.

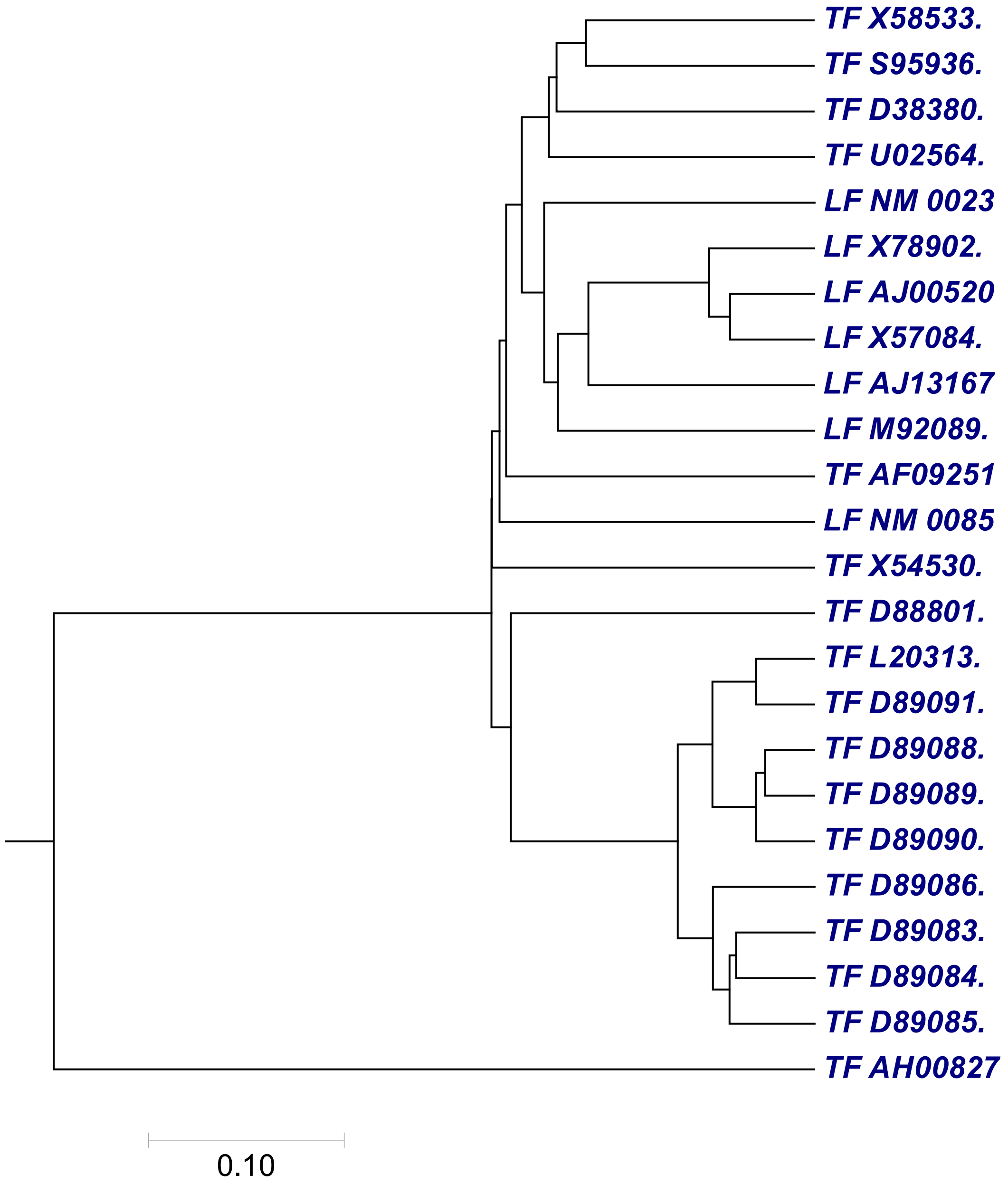

Figure 51: FFP method using string length 7.

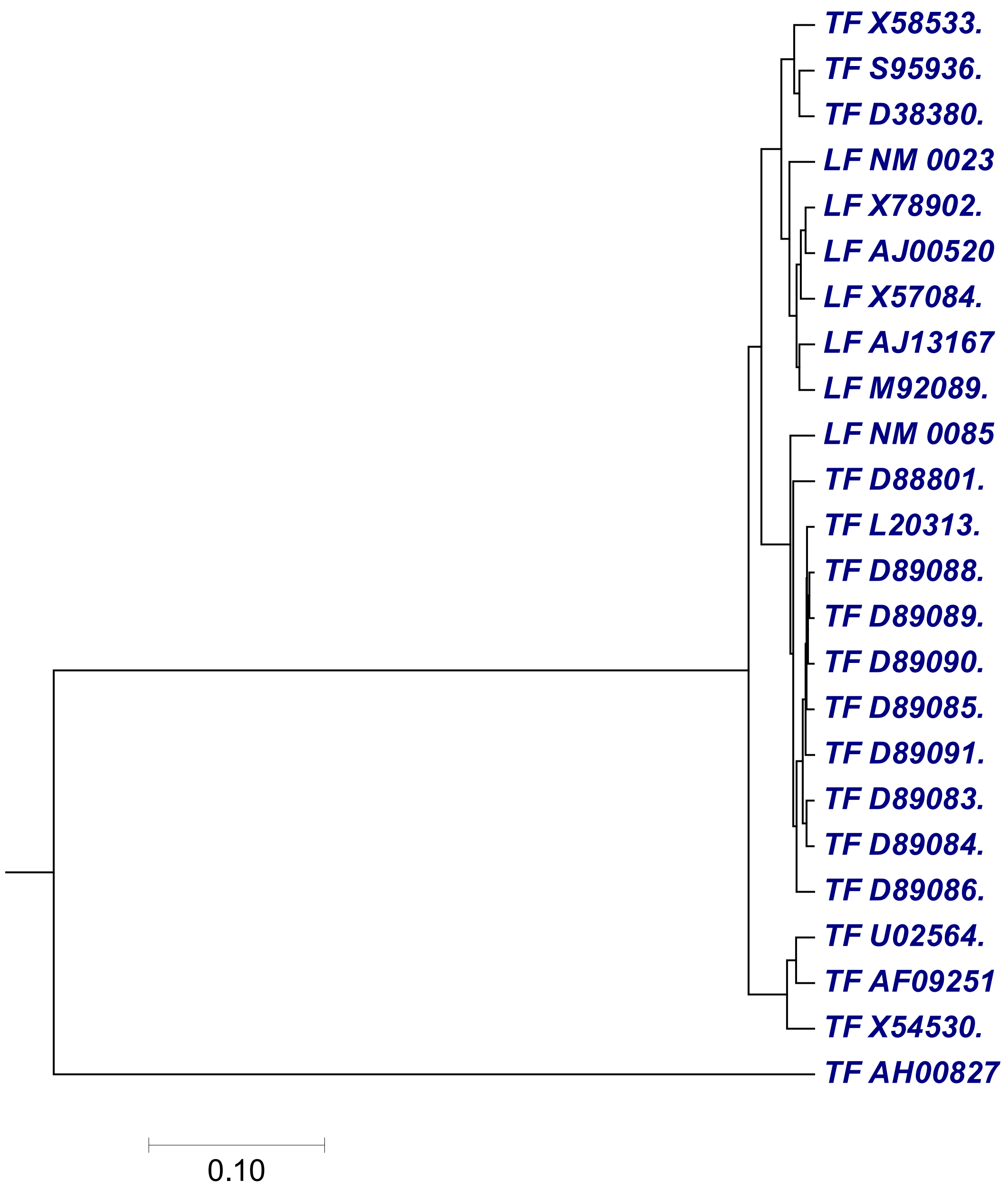

Figure 52: RTD method using string length 1.

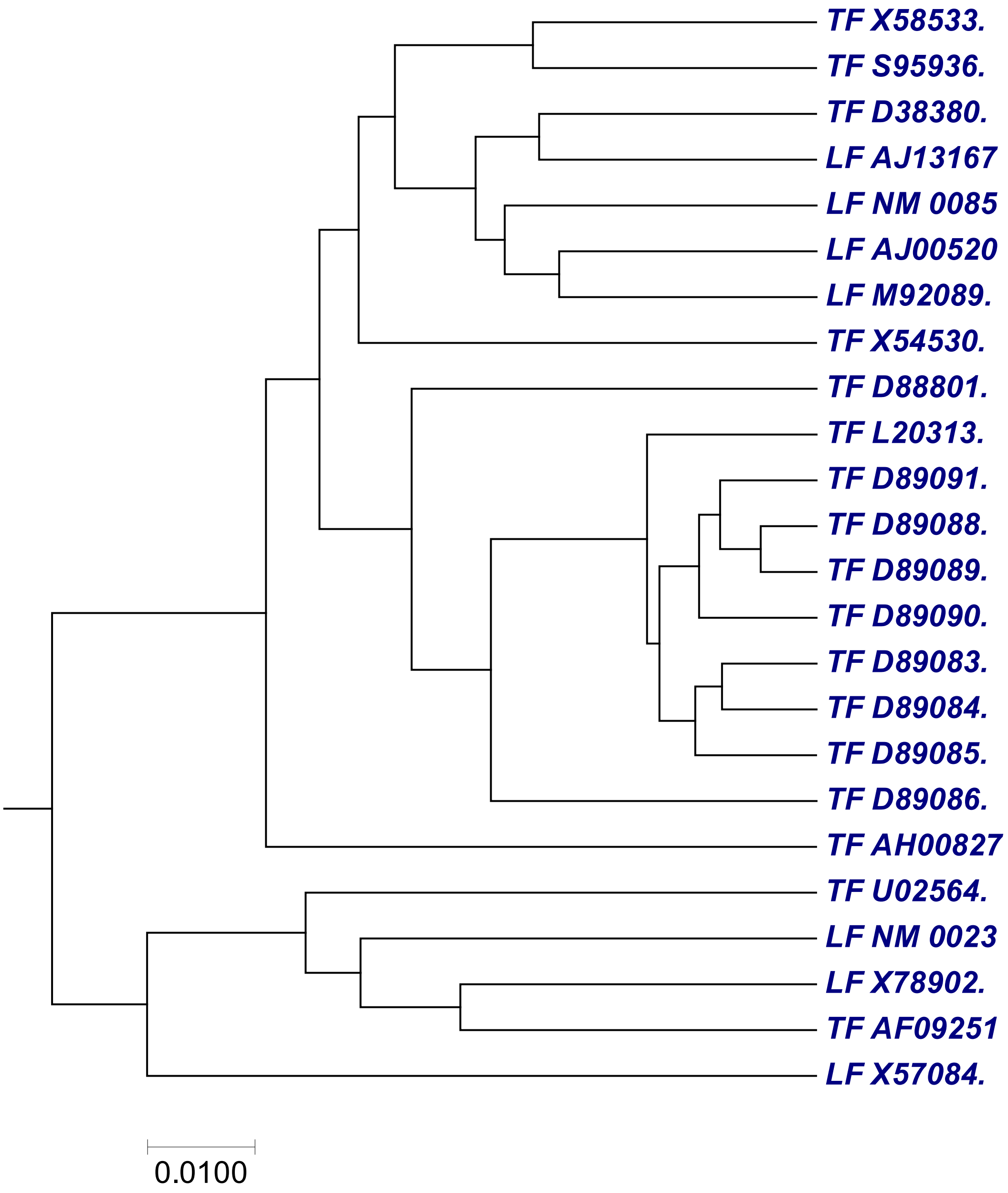

Figure 53: BBC method.

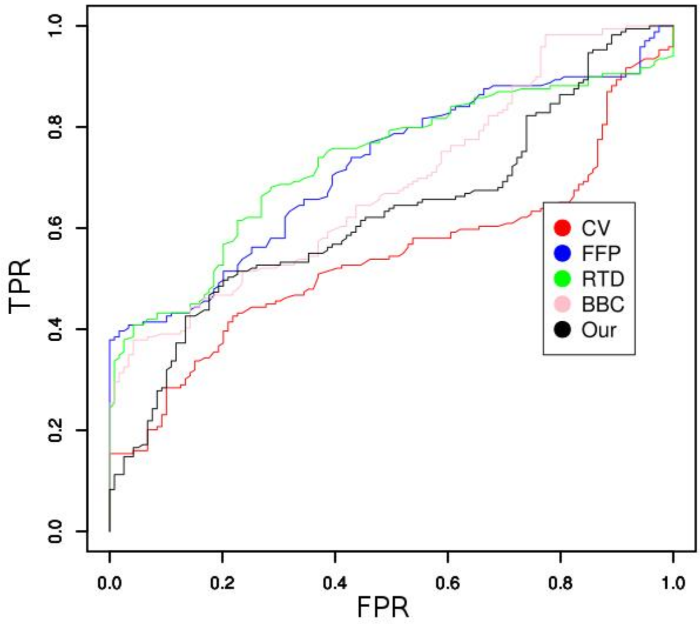

Dataset→ 24 Eutherian mammal		
Methods↓	**AUC↓**	**Running time↓**
CV method	0.539058	<1s
FFP method	0.717816	<1s
RTD method	0.727413	<1s
BBC method	0.685147	<1s
Our method	0.627617	<1s

Figure 54: Receiver operating characteristic curve (ROC) and Area under the ROC Curve on 24 Eutherian mammal sequences.

As shown in Figure 49 generated by our method, we can observe that all transferrin sequences (red) were clustered into two distinct clades, except rabbit transferrin sequence which was grouped with lactoferrin class. Similarly, all lactoferrin sequences (green) were clustered together, except mouse lactoferrin sequence which was grouped with transferrin class. However, the trees (Figures 50, 51, 52 and 53) generated by other methods could not cluster the sequences properly as our method. Moreover, the AUC of our method is 0.63 (Figure 54).

Phylogenetic tree on 40 bacterial isolates sequences.

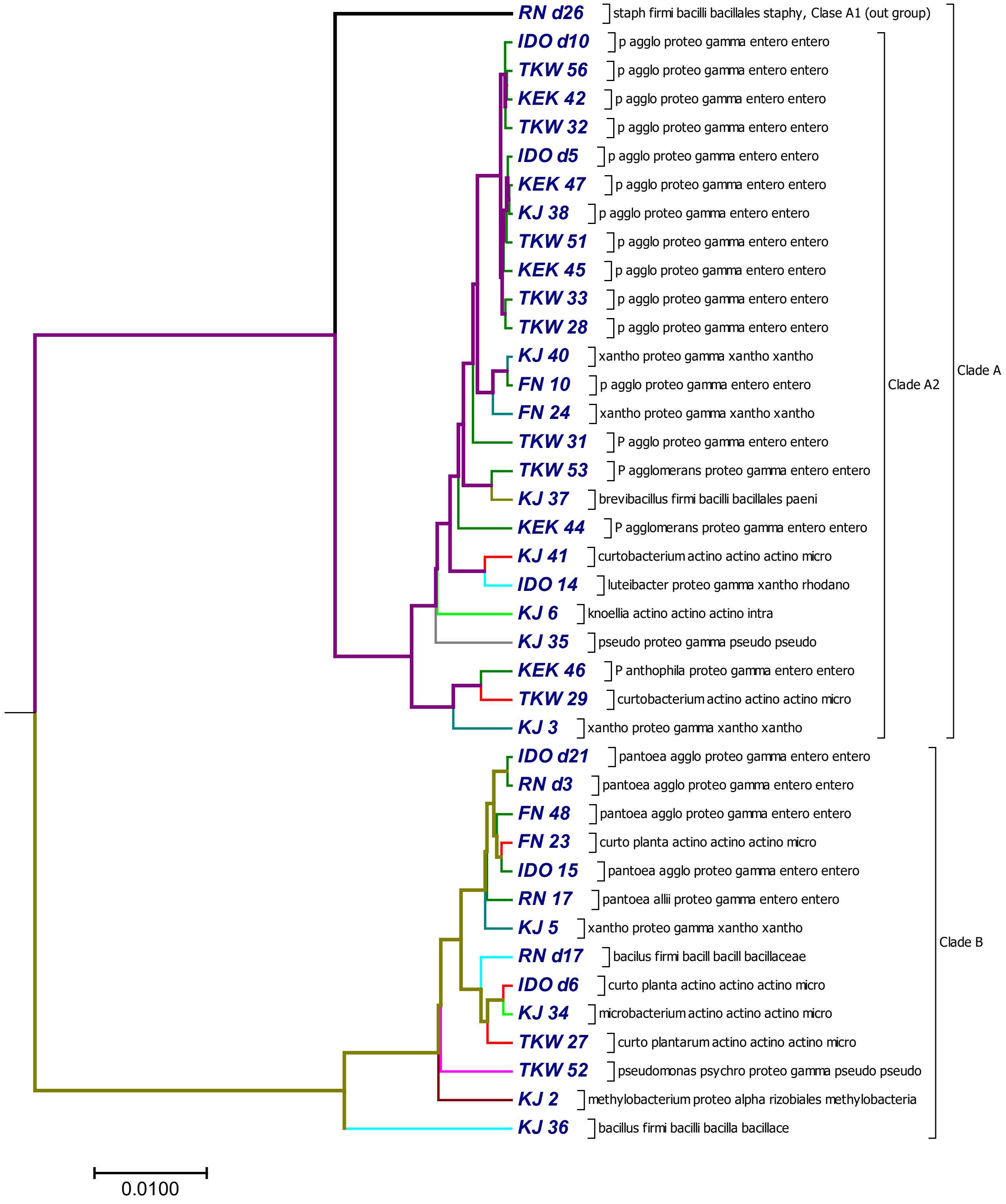
RN d26 staph firmi bacilli bacillales staphy, Clase A1 (out group)
IDO d10 p agglo proteo gamma entero entero
TKW 56 p agglo proteo gamma entero entero
KEK 42 p agglo proteo gamma entero entero
TKW 32 p agglo proteo gamma entero entero
IDO d5 p agglo proteo gamma entero entero
KEK 47 p agglo proteo gamma entero entero
KJ 38 p agglo proteo gamma entero entero
TKW 51 p agglo proteo gamma entero entero
KEK 45 p agglo proteo gamma entero entero
TKW 33 p agglo proteo gamma entero entero
TKW 28 p agglo proteo gamma entero entero
KJ 40 xantho proteo gamma xantho xantho
FN 10 p agglo proteo gamma entero entero
FN 24 xantho proteo gamma xantho xantho
TKW 31 P agglo proteo gamma entero entero
TKW 53 P agglomerans proteo gamma entero entero
KJ 37 brevibacillus firmi bacilli bacillales paeni
KEK 44 P agglomerans proteo gamma entero entero
KJ 41 curtobacterium actino actino actino micro
IDO 14 luteibacter proteo gamma xantho rhodano
KJ 6 knoellia actino actino actino intra
KJ 35 pseudo proteo gamma pseudo pseudo
KEK 46 P anthophila proteo gamma entero entero
TKW 29 curtobacterium actino actino actino micro
KJ 3 xantho proteo gamma xantho xantho
IDO d21 pantoea agglo proteo gamma entero entero
RN d3 pantoea agglo proteo gamma entero entero
FN 48 pantoea agglo proteo gamma entero entero
FN 23 curto planta actino actino actino micro
IDO 15 pantoea agglo proteo gamma entero entero
RN 17 pantoea allii proteo gamma entero entero
KJ 5 xantho proteo gamma xantho xantho
RN d17 bacilus firmi bacill bacill bacillaceae
IDO d6 curto planta actino actino actino micro
KJ 34 microbacterium actino actino actino micro
TKW 27 curto plantarum actino actino actino micro
TKW 52 pseudomonas psychro proteo gamma pseudo pseudo
KJ 2 methylobacterium proteo alpha rizobiales methylobacteria
KJ 36 bacillus firmi bacilli bacilla bacillace
Clade A2
Clade A
Clade B
0.0100

Figure 55: Our method.

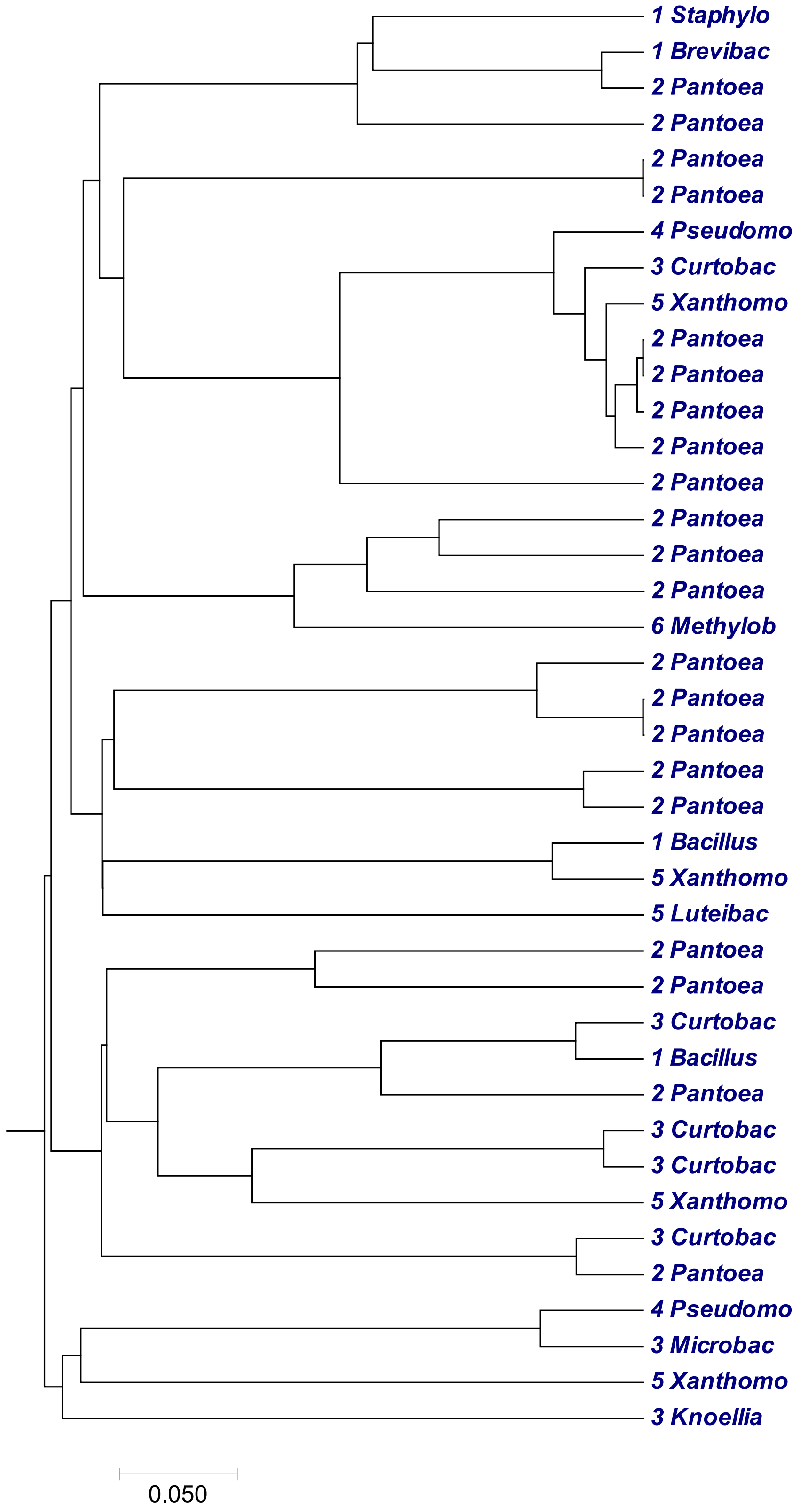

Figure 56: CV method using string length 3.

1 →Bacillales, 2→Enterobacteriales, 3→Actinomycetales, 4→Pseudomonadales, 5→Xanthomonadales, 6→Rhizobiales.

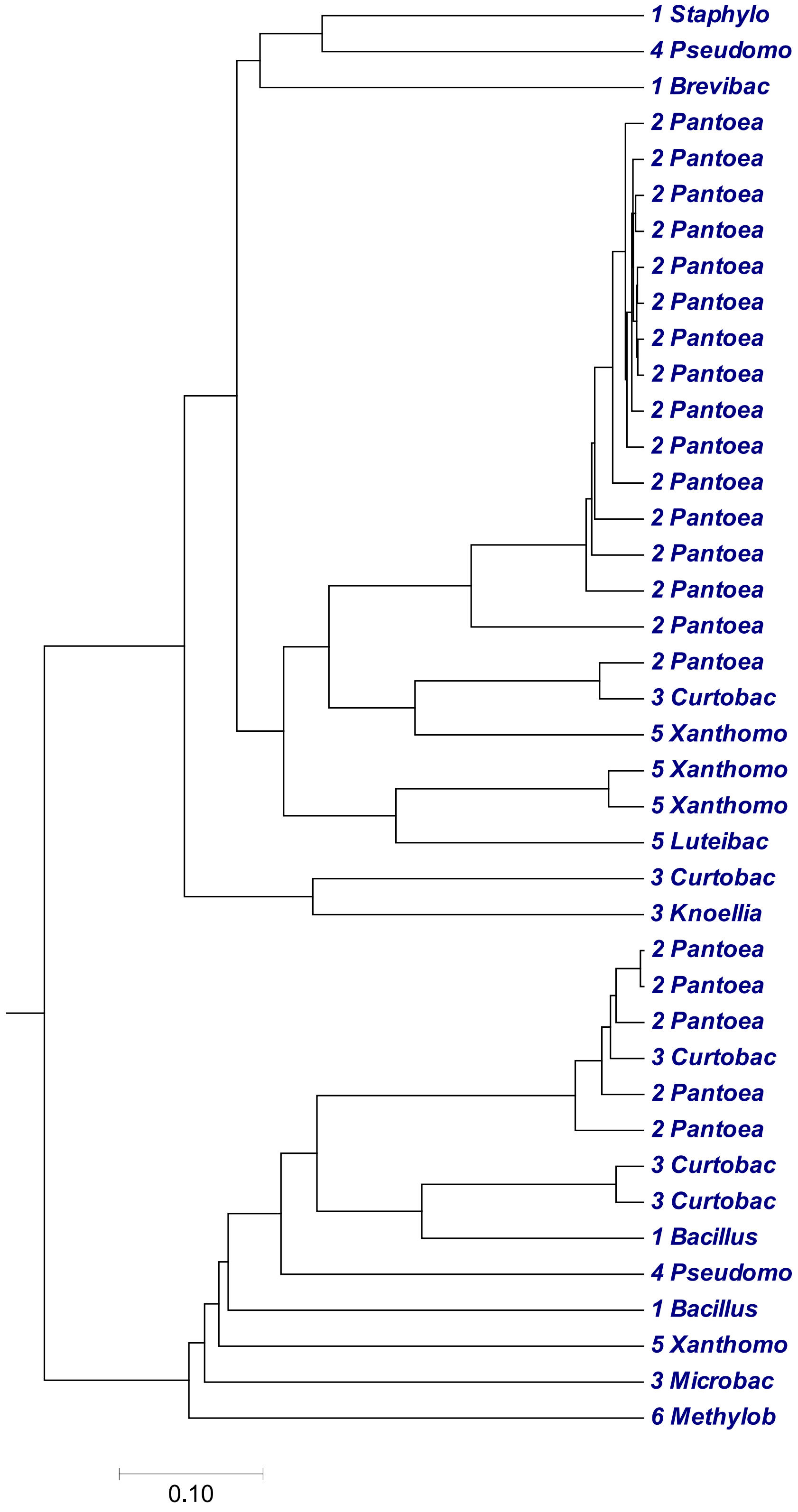

Figure 57: FFP method using string length 7.

1 →Bacillales, 2→Enterobacteriales, 3→Actinomycetales, 4→Pseudomonadales, 5→Xanthomonadales, 6→Rhizobiales.

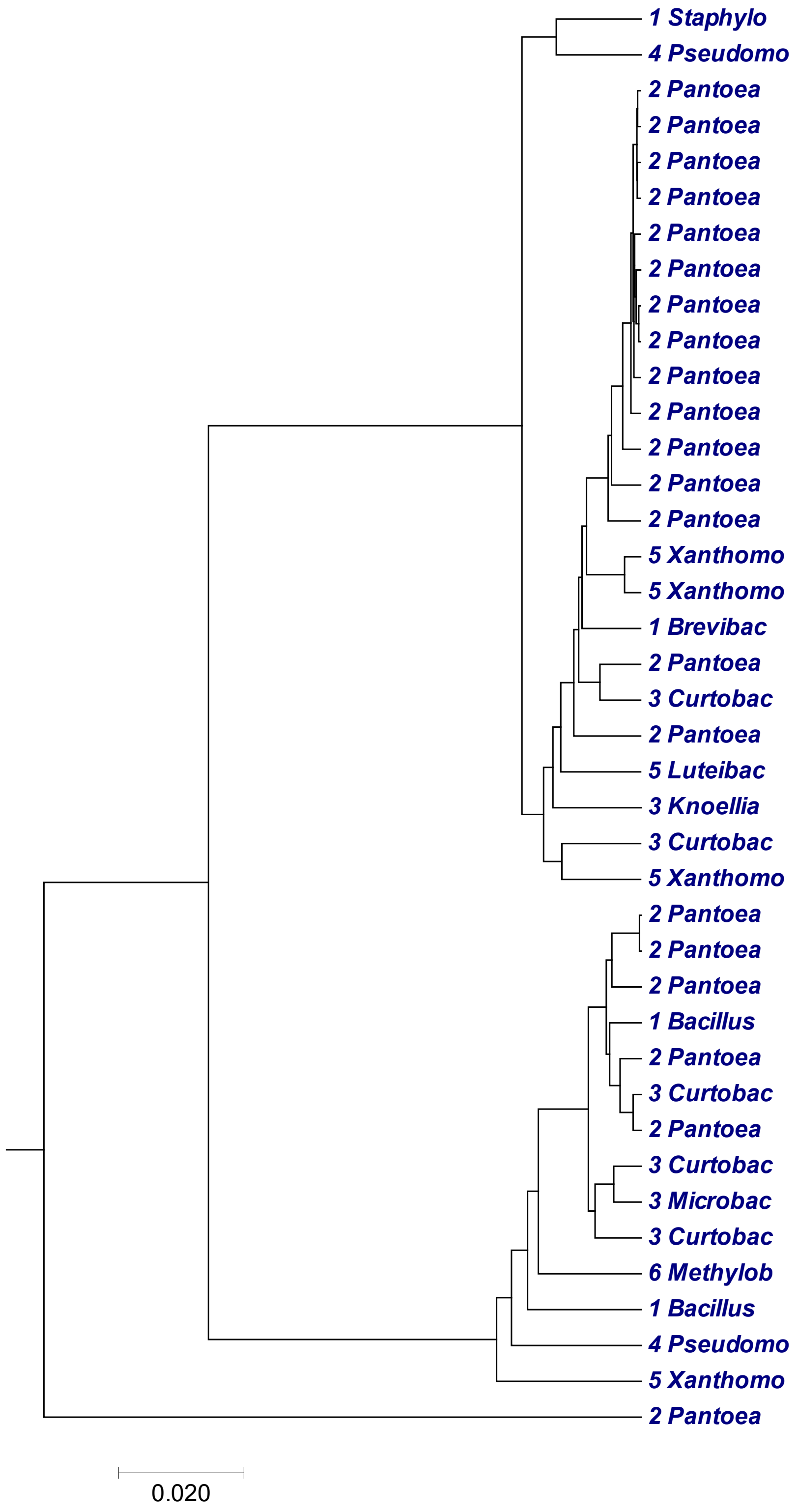

Figure 58: RTD method using string length 1.

1 →Bacillales, 2→Enterobacteriales, 3→Actinomycetales, 4→Pseudomonadales, 5→Xanthomonadales, 6→Rhizobiales.

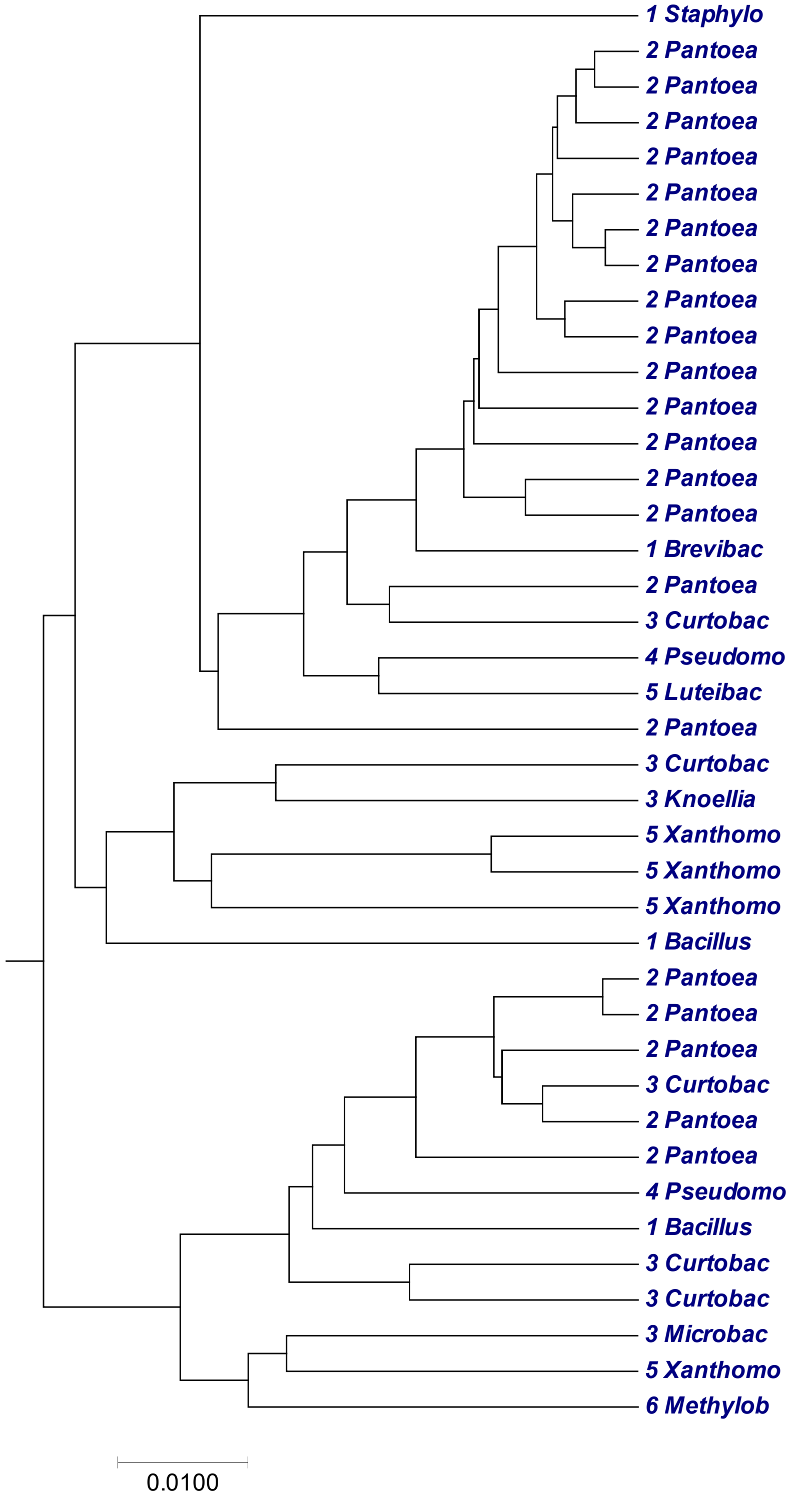

Figure 59: BBC method.

1 →Bacillales, 2→Enterobacteriales, 3→Actinomycetales, 4→Pseudomonadales, 5→Xanthomonadales, 6→Rhizobiales.

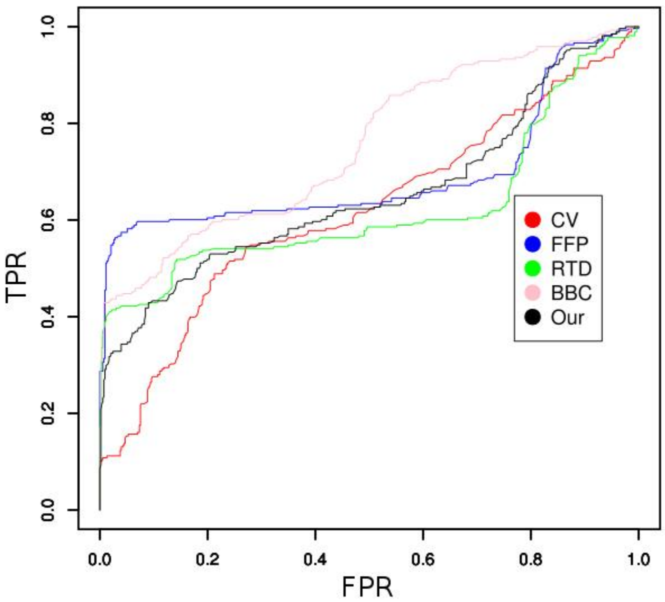

Dataset→	40 bacterial isolates	
Methods↓	AUC↓	Running time↓
CV method	0.618372	<1s
FFP method	0.692213	<1s
RTD method	0.624117	<1s
BBC method	0.756011	<1s
Our method	0.653343	<1s

Figure 60: Receiver operating characteristic curve (ROC) and Area under the ROC Curve on 40 bacterial isolates sequences.

Our 40 bacterial sequences belong to 11 genera and 16 species. We compared our method with four different techniques and observed little variation in their clustering pattern (Fig. 55-60) except CV method. The 40 bacterial species for AUC were numbered at order level and all the methods except CV, clustered order Enterobacteriales alike. AUC values from the five approaches range from 0.618 to 0.756 with the lowest for method CV and highest for BBC. Although BBC method has the highest AUC value but its clustering pattern to similar to our method (AUC=0.653).

Reference:

1. Zielezinski, A., Vinga, S., Almeida, J. & Karlowski, W. M. Alignment-free sequence comparison: benefits, applications, and tools. Genome Biol. 18, 186 (2017).
2. Swets, J. Measuring the accuracy of diagnostic systems. Sci. 240, 1285–1293 (1988).
3. NEMES, S. & HARTEL, T. Summary measures for binary classification systems in animal ecology. North-Western J. Zool. 6, 323–330 (2010).
4. Siriussawakul, A. et al. Predictive performance of a multivariable difficult intubation model for obese patients. PLOS ONE 1–15 (2018).
5. Antognoli, M. C. et al. Analysis of the diagnostic accuracy of the gamma interferon assay for detection of bovine tuberculosis in u.s. herds. Prev. Vet. Medicine 101, 35 – 41 (2011).
6. Zhu, W., Zeng, N. & Wang, N. Sensitivity, specificity, accuracy, associated confidence interval and roc analysis with practical SAS implementations. in Proceedings of the NESUG Health Care and Life Sciences, Baltimore, Md, USA (2010).
7. Felsenstein, J. Phylip–phylogeny inference package(version 3.2). Cladistics 5 164–166 (1989).
8. Sonego, P., Kocsor, A. & Pongor, S. Roc analysis: applications to the classification of biological sequences and 3d structures. Briefings Bioinforma. 9, 198–209 (2008).